at odds with past brain imaging studies showing that nonwords relative to words produced greater activation in the left prefrontal area, whereas the opposite contrast produced either no activation difference at all (Rumsey et al., 1997) or activation difference in several distinct areas of the left hemisphere, including the fusiform (Herbster et al., 1997) and middle temporal gyri (Fiebach et al., 2002) and inferior frontal area (Fiez et al., 1999).

However, another line of evidence supporting the hypothesized dual neural systems for reading is available from the neuropsychological literature on the two polarized forms of acquired reading disorder, surface and phonological dyslexia. The former is thought to reflect a selective impairment of the whole-word reading system and is most frequently associated with damage to the left superior temporal area, whereas the latter arises from a selective impairment of the orthography-to-phonology conversion procedure and is associated with the angular and supramarginal gyri in the left hemisphere (Friedmann et al., 1993; Greenwald, 2001). In fact, it is possible that some past neuroimaging studies have failed to detect the effect of lexicality because brain activation triggered by the conscious perception of word-like stimuli should be subject to the top-down attentional amplification by the prefrontal cortex. This in turn produces a distributed activation of the fronto-temporo-parietal network, thereby causing an underestimation of the potential activation difference between words and nonwords. The combined use of visual masking and TMS may have allowed dissection of the cerebral correlates of the conventional dual-route model for reading by eliminating such top-down modification of the activation of these task-specific posterior brain areas.

Experimental Procedures

Participants

Fourteen native Japanese speakers (age range 22–37 years) volunteered to participate in Experiment 1. A separate group of 16 right-handed, native Japanese speakers (age range 20–41 years) were recruited for Experiment 2. None of them had a previous history of neurological or psychiatric disease. All participants gave written informed consent prior to the TMS experiment. The protocol of this study was approved by the ethical committee of the University of Tokyo Graduate School of Medicine.

Stimuli and Task

The stimulus materials consisted of 20 trisyllabic words spelled with three characters in kana script (Japanese syllabary) and 20 trisyllabic nonwords created by rearranging the character-string of the real word items. A set of 160 prime-target pairs was constructed such that each item appeared twice as a visual target preceded either by itself or a different item in the same modality in "within-modal" trials, and twice as an auditory target preceded either by the same or a different item in the visual modality in "cross-modal" trials. The lexical status of primes was always congruent with that of targets both for the within- and cross-modal conditions.

The sequence of events used for the present experiment is illustrated in Figure 1. In cross-modal trials, the auditory targets were presented synchronously with a backward mask which consisted of a random combination of four pseudo-characters (∈,∩,∋,∪). The within- and cross-modal trials were randomly intermixed in the same experimental session such that the modality of a given target was unpredictable prior to its appearance (Kouider and Dupoux, 2001). For the LD task, participants determined whether or not the target words irrespective of their modality represented a real Japanese word as quickly and as accurately as possible, whereas for the PRN task they read aloud the visual targets or repeated the auditory targets as quickly as possible. After a brief training session, participants received four TMS sessions, each lasting 480 s for each task for each stimulation site. The effects of task order and stimulation sites were counterbalanced across participants. The experiment was arranged in a 2 × 2 by 2 × 2 factorial design in which the main factors of interest were prime-target relation (identical versus unrelated), modality (within- versus cross-), lexicality (words versus nonwords), and stimulation site (L-STG versus L-IPL).

TMS Procedures

A high-resolution anatomical MRI scan was obtained for each participant prior to the main experiment. The target sites for TMS were localized for each participant using a computerized stereotaxic system (Eximia Navigated Brain Stimulation [NBS] System, Nexstim, Finland). For the L-STG stimulation, we targeted a middle part of the left lateral temporal cortex ~15 mm posterior to the lateral edge of the primary auditory cortex or transverse temporal gyrus, keeping a spatial separation of ~20 mm from the left occipitotemporal area associated with visual word form recognition (Cohen et al., 2000). The L-IPL was located at the left inferior parietal lobule on the lower bank of the left intraparietal sulcus corresponding to Brodmann's area 40 (Price, 1998). The mean coordinates of the two anatomical targets across participants were mapped onto the standardized brain space by the Montreal Neurological Institute using affine transformation of the individual brain (Figure 3A and Figure 4A).

A single-pulse TMS was delivered in each trial using two MagStim 200 magnetic stimulators connected to a 70 mm figure-of-eight coil through a BiStim module (Magstim, UK). The magnetic pulse has a rise time of 100 ms and a duration of 1 ms, whereas the effects in the underlying cortical region are estimated to last approximately 10 ms (Ilmoniemi et al., 1997). The coil was kept tangential to the skull for stimulating the IPL and STS with the handle pointing backward parallel to the midline. In each trial, a single pulse synchronized to the onset of the fixation point (see Figure 1) was applied to the target anatomical structure at an intensity of 70% of the generator's total power output, which corresponds to approximately 90%–130% of the motor threshold for the resting hand muscles. The spatial extent of the induced electric field was estimated as a cone-shaped distribution within a diameter of 10 mm at a depth of 10 mm from the coil center.

The real-time NBS system tracked the position and orientation of the coil and the head at a rate of ~20 Hz, allowing us to minimize their mutual displacement during the TMS session. For each TMS pulse, this 3D monitoring system also computed and recorded the estimated distribution and strength of the intracranial electric field induced by the stimulation using a conventional multilayer spherical approximation (e.g., Roth et al., 1991; Sarvas, 1987). For each participant, the spatial displacement of stimulation points was then calculated for each anatomical target by computing average root mean square distance of the trial-by-trial estimated maximum electric field relative to the initial stimulation point.

Acknowledgments

We are grateful to three anonymous reviewers for constructive comments on an earlier version of this manuscript. We also thank Takeshi Uehara for technical assistance. This work was supported by the Nakayama Foundation for Human Sciences, a Grant-in-Aid for Young Scientists (B) 15700252 by the Japan Ministry of Education, Culture, Sports, Science and Technology (K.N.), and Research Project Grant-in-aid for Scientific Research No. 17590865 (R.H.) and No. 16500194 (Y.U.), also from the Japan Ministry of Education, Culture, Sports, Science and Technology.

Received: May 18, 2006
Revised: August 4, 2006
Accepted: September 19, 2006
Published: November 8, 2006

References

Beauchamp, M.S., Argall, B.D., Bodurka, J., Duyn, J.H., and Martin, A. (2004). Unraveling multisensory integration: patchy organization within human STS multisensory cortex. Nat. Neurosci. 7, 1190–1192.

Beauchamp, M.S. (2005). See me, hear me, touch me: multisensory integration in lateral occipital-temporal cortex. Curr. Opin. Neurobiol. *15*, 145–153.

Bitan, T., Booth, J.R., Choy, J., Burman, D.D., Gitelman, D.R., and Mesulam, M.M. (2005). Shifts of effective connectivity within a language network during rhyming and spelling. J. Neurosci. *25*, 5397–5403.

Bokde, A.L., Tagamets, M.A., Friedman, R.B., and Horwitz, B. (2001). Functional interactions of the inferior frontal cortex during the processing of words and word-like stimuli. Neuron *30*, 609–617.

Catani, M., Jones, D.K., Donato, R., and Ffytche, D.H. (2003). Occipito-temporal connections in the human brain. Brain *126*, 2093–2107.

Cohen, L., Dehaene, S., Naccache, L., Lehericy, S., Dehaene-Lambertz, G., Henaff, M.A., and Michel, F. (2000). The visual word form area: spatial and temporal characterization of an initial stage of reading in normal subjects and posterior split-brain patients. Brain *123*, 291–307.

Cohen, L., Jobert, A., Le Bihan, D., and Dehaene, S. (2004). Distinct unimodal and multimodal regions for word processing in the left temporal cortex. Neuroimage *23*, 1256–1270.

Coltheart, M., Rastle, K., Perry, C., Langdon, R., and Ziegler, J. (2001). DRC: a dual route cascaded model of visual word recognition and reading aloud. Psychol. Rev. *108*, 204–256.

Dehaene, S., Kerszberg, M., and Changeux, J.P. (1998). A neuronal model of a global workspace in effortful cognitive tasks. Proc. Natl. Acad. Sci. USA *95*, 14529–14534.

Dehaene, S., Naccache, L., Cohen, L., Bihan, D.L., Mangin, J.F., Poline, J.B., and Riviere, D. (2001). Cerebral mechanisms of word masking and unconscious repetition priming. Nat. Neurosci. *4*, 752–758.

Dehaene, S., Jobert, A., Naccache, L., Ciuciu, P., Poline, J.B., Le Bihan, D., and Cohen, L. (2004). Letter binding and invariant recognition of masked words: behavioral and neuroimaging evidence. Psychol. Sci. *15*, 307–313.

Demonet, J.F., Chollet, F., Ramsay, S., Cardebat, D., Nespoulous, J.L., Wise, R., Rascol, A., and Frackowiak, R. (1992). The anatomy of phonological and semantic processing in normal subjects. Brain *115*, 1753–1768.

Fiebach, C.J., Friederici, A.D., Muller, K., and von Cramon, D.Y. (2002). fMRI evidence for dual routes to the mental lexicon in visual word recognition. J. Cogn. Neurosci. *14*, 11–23.

Fiez, J.A., Balota, D.A., Raichle, M.E., and Petersen, S.E. (1999). Effects of lexicality, frequency, and spelling-to-sound consistency on the functional anatomy of reading. Neuron *24*, 205–218.

Forster, K.I., and Davis, C. (1991). The density constraint on form-priming in the naming task: Interference effects from a masked prime. J. Mem. Lang. *30*, 1–25.

Forster, K.I., Mohan, K., and Hector, J. (2003). The mechanics of masked priming. In Masked Priming: State of the Art, S. Kinoshita and S.J. Lupker, eds. (New York: Psychology Press), pp. 3–37.

Friedmann, R., Ween, J.E., and Albert, M.L. (1993). Alexia. In Clinical Neuropsychology, K.M. Heilmann and E. Valenstein, eds. (New York: Oxford University Press), pp. 37–62.

Frost, R. (2003). The robustness of phonological effects in fast priming. In Masked Priming: The State of the Art, S. Kinoshita and S.J. Lupker, eds. (New York: Psychology Press), pp. 173–191.

Fuster, J.M. (1997). The Prefrontal Cortex: Anatomy, Physiology and Neuropsychology of the Frontal Lobe, Third Edition (New York: Lippincott-Raven).

Grainger, J., Diependaele, K., Spinelli, E., Ferrand, L., and Farioli, F. (2003). Masked repetition and phonological priming within and across modalities. J. Exp. Psychol. Learn. Mem. Cogn. *29*, 1256–1269.

Greenwald, M. (2001). Acquired reading disorders. In Handbook of Neuropsychology: Language and Aphasia, R.S. Berndt, J. Grafman, and F. Boller, eds. (Amsterdam: Elsevier), pp. 205–220.

Henson, R.N., Shallice, T., and Dolan, R. (2000). Neuroimaging evidence for dissociable forms of repetition priming. Science *287*, 1269–1272.

Herbster, A.N., Mintun, M.A., Nebes, R.D., and Becker, J.T. (1997). Regional cerebral blood flow during word and nonword reading. Hum. Brain Mapp. *5*, 84–92.

Horwitz, B., Rumsey, J.M., and Donohue, B.C. (1998). Functional connectivity of the angular gyrus in normal reading and dyslexia. Proc. Natl. Acad. Sci. USA *95*, 8939–8944.

Howard, D., Patterson, K., Wise, R., Brown, W.D., Friston, K., Weiller, C., and Frackowiak, R. (1992). The cortical localization of the lexicons. Positron emission tomography evidence. Brain *115*, 1769–1782.

Ilmoniemi, R.J., Virtanen, J., Ruohonen, J., Karhu, J., Aronen, H.J., Naatanen, R., and Katila, T. (1997). Neuronal responses to magnetic stimulation reveal cortical reactivity and connectivity. Neuroreport *8*, 3537–3540.

Kinoshita, S. (2003). The nature of masked onset priming effects in naming: a review. In Masked Priming: The State of the Art, S. Kinoshita and S.J. Lupker, eds. (New York: Psychology Press), pp. 223–240.

Kouider, S., and Dupoux, E. (2001). A functional disconnection between spoken and visual word recognition: evidence from unconscious priming. Cognition *82*, B35–B49.

Lamme, V.A. (2003). Why visual attention and awareness are different. Trends Cogn. Sci. *7*, 12–18.

Lamme, V.A., Zipser, K., and Spekreijse, H. (2002). Masking interrupts figure-ground signals in V1. J. Cogn. Neurosci. *14*, 1044–1053.

Lerner, Y., Hendler, T., Ben-Bashat, D., Harel, M., and Malach, R. (2001). A hierarchical axis of object processing stages in the human visual cortex. Cereb. Cortex *11*, 287–297.

Mechelli, A., Crinion, J.T., Long, S., Friston, K.J., Lambon Ralph, M.A., Patterson, K., McClelland, J.L., and Price, C.J. (2005). Dissociating reading processes on the basis of neuronal interactions. J. Cogn. Neurosci. *17*, 1753–1765.

Miller, E.K., and Cohen, J.D. (2001). An integrative theory of prefrontal cortex function. Annu. Rev. Neurosci. *24*, 167–202.

Naccache, L., Blandin, E., and Dehaene, S. (2002). Unconscious masked priming depends on temporal attention. Psychol. Sci. *13*, 416–424.

Nobre, A.C., Allison, T., and McCarthy, G. (1994). Word recognition in the human inferior temporal lobe. Nature *372*, 260–263.

Paulesu, E., McCrory, E., Fazio, F., Menoncello, L., Brunswick, N., Cappa, S.F., Cotelli, M., Cossu, G., Corte, F., Lorusso, M., et al. (2000). A cultural effect on brain function. Nat. Neurosci. *3*, 91–96.

Price, C.J. (1998). The functional anatomy of word comprehension and production. Trends Cogn. Sci. *2*, 281–288.

Price, C.J., Wise, R.J., and Frackowiak, R.S. (1996). Demonstrating the implicit processing of visually presented words and pseudowords. Cereb. Cortex *6*, 62–70.

Ramachandran, V.S., and Cobb, S. (1995). Visual attention modulates metacontrast masking. Nature *373*, 66–68.

Roth, B.J., Saypol, J.M., Hallett, M., and Cohen, L.G. (1991). A theoretical calculation of the electric field induced in the cortex during magnetic stimulation. Electroencephalogr. Clin. Neurophysiol. *81*, 47–56.

Rumsey, J.M., Horwitz, B., Donohue, B.C., Nace, K., Maisog, J.M., and Andreason, P. (1997). Phonological and orthographic components of word recognition. A PET-rCBF study. Brain *120*, 739–759.

Sarvas, J. (1987). Basic mathematical and electromagnetic concepts of the biomagnetic inverse problem. Phys. Med. Biol. *32*, 11–22.

Shaywitz, S.E., Shaywitz, B.A., Pugh, K.R., Fulbright, R.K., Constable, R.T., Mencl, W.E., Shankweiler, D.P., Liberman, A.M., Skudlarski, P., Fletcher, J.M., et al. (1998). Functional disruption in the organization of the brain for reading in dyslexia. Proc. Natl. Acad. Sci. USA *95*, 2636–2641.

Talairach, J., and Tournoux, P. (1988). Co-Planar Stereotaxic Atlas of the Human Brain: 3-D Proportional System: an Approach to Cerebral Imaging (New York: Thieme Medical Publishers).

Tarkiainen, A., Helenius, P., Hansen, P.C., Cornelissen, P.L., and Salmelin, R. (1999). Dynamics of letter string perception in the human occipitotemporal cortex. Brain *122*, 2119–2132.

van Turennout, M., Ellmore, T., and Martin, A. (2000). Long-lasting cortical plasticity in the object naming system. Nat. Neurosci. *3*, 1329–1334.

Wright, T.M., Pelphrey, K.A., Allison, T., McKeown, M.J., and McCarthy, G. (2003). Polysensory interactions along lateral temporal regions evoked by audiovisual speech. Cereb. Cortex *13*, 1034–1043.

ELSEVIER

Clinical Neurophysiology 118 (2007) 877–886

www.elsevier.com/locate/clinph

Median nerve somatosensory evoked potentials and their high-frequency oscillations in amyotrophic lateral sclerosis ☆

Masashi Hamada, Ritsuko Hanajima, Yasuo Terao, Fumio Sato, Tomoko Okano, Kaoru Yuasa, Toshiaki Furubayashi, Shingo Okabe, Noritoshi Arai, Yoshikazu Ugawa *

Department of Neurology, Division of Neuroscience, Graduate School of Medicine, The University of Tokyo, 7-3-1, Hongo, Bunkyo-ku, Tokyo 113-8655, Japan

Accepted 5 December 2006
Available online 16 February 2007

Abstract

Objective: To investigate sensory cortical changes in amyotrophic lateral sclerosis (ALS), we studied somatosensory evoked potentials (SEPs) and their high-frequency oscillation potentials.
Methods: Subjects were 15 healthy volunteers and 26 ALS patients. Median nerve SEPs were recorded and several peaks of oscillations were obtained by digitally filtering raw SEPs. The patients were sorted into three groups according to the level of weakness of abductor pollicis brevis muscle (APB): mild, moderate and severe. The latencies and amplitudes of main and oscillation components of SEP were compared among normal subjects and the three patient groups.
Results: The early cortical response was enlarged in the moderate weakness group, while it was attenuated in the severe weakness group. No differences were noted in the size ratios of oscillations to the main SEP component between the patients and normal subjects. The central sensory conduction time (CCT) and N20 duration were prolonged in spite of normal other latencies.
Conclusions: The median nerve SEP amplitude changes are associated with motor disturbances in ALS. The cortical potential enhancement of SEPs with moderate weakness in ALS may reflect some compensatory function of the sensory cortex for motor disturbances.
Significance: The sensory cortical compensation for motor disturbances is shown in ALS, which must be important information for rehabilitation.

Keywords: Somatosensory evoked potential; High-frequency oscillation; Amyotrophic lateral sclerosis

1. Introduction

Somatosensory evoked potentials (SEPs) have been studied in amyotrophic lateral sclerosis (ALS): some reports revealed no SEP abnormalities (Cascino et al., 1988; Chiappa, 1983; Oh et al., 1985), while others showed abnormalities in upper limb SEPs (Bosch et al., 1985; Cosi et al., 1984; Dasheiff et al., 1985; Radtke et al., 1986; Subramaniam and Yiannikas, 1990; Theys et al., 1999; Zanette et al., 1990) and lower limb SEPs (Georgesco et al., 1997; Matheson et al., 1986; Radtke et al., 1986; Subramaniam and Yiannikas, 1990; Zanette et al., 1996). They are still controversial.

The high-frequency oscillation (HFO), one newly developed SEP analysis, is considered to reflect some sensory cortical information processing. The N20 potential is considered to reflect an initial excitation of neurons in area 3b (Allison et al., 1991; Tiihonen et al., 1989). In contrast, the generators of HFOs remain to be determined, even though several candidates have been proposed; such as brainstem, thalamus, thalamocortical presynaptic action potentials and somatosensory cortex (Curio et al., 1997; Eisen et al., 1984; Gobbelé et al., 1998, 2004; Hashimoto et al., 1996, 1999; Klostermann et al., 2002; Shimazu et al., 2000). We

☆ Disclosure: The authors have reported no conflicts of interest.
* Corresponding author. Tel.: +81 3 5800 8672; fax: +81 3 5800 6548.
E-mail address: ugawa-tky@umin.net (Y. Ugawa).

1388-2457/$32.00
doi:10.1016/j.clinph.2006.12.001

previously reported changes in HFOs in movement disorders (Mochizuki et al., 1999). However, the high-frequency oscillations (HFOs) of median nerve SEP have not been studied in ALS.

In addition, several studies using transcranial magnetic stimulation (TMS) showed that pure sensory input facilitated the primary motor cortex (M1) (Hamdy et al., 1998; Kaelin-Lang et al., 2002; Ridding et al., 2000; Rosenkranz and Rothwell, 2003; Rosenkranz and Rothwell, 2004; Terao et al., 1995, 1999) and a number of gating studies confirmed an attenuation of the early cortical responses to median nerve stimulation by motor interferences (Gobbelé et al., 2003; Kakigi et al., 1995; Mochizuki et al., 2004; Rossini et al., 1999; Tanosaki et al., 2002; Valeriani et al., 1999). These reports indicate there are several kinds of interactions between the motor and sensory systems in humans. Those integrations of the sensorimotor information must be necessary for precise and purposeful movements.

One functional magnetic resonance imaging study revealed cortical reorganization in ALS (Konrad et al., 2002). They concluded that a partial compensation between motor areas was a strategy to optimize motor performances in ALS. We hypothesize that similar compensation for motor dysfunction might occur in the somatosensory system in ALS.

To solve the above-mentioned three issues; (1) the inconsistency of SEP results, (2) the lack of HFO studies, (3) sensory compensation for weakness, in the present communication, we studied median nerve SEPs in patients with ALS.

2. Subjects and methods

2.1. Subjects

We studied 26 patients with ALS. The diagnosis was based on the revised El Escorial criteria (Brooks et al., 2000): 15 had definite, five probable, and six probable-laboratory-supported ALS at the time of the examination. Their clinical features are summarized in Table 1. The age ranged from 33 to 78 years (mean ± SD; 62.1 ± 10.2 years). The duration of the illness at the time of our experiment ranged from 3 to 48 months (16.7 ± 15.9 months).

Table 1
Clinical characteristics of the patients F, female: M, male

Case No.	Age (year)	Sex	Disease duration (months)	El Escorial criteria	Clinical onset	Recorded side	Severity
1	33	M	7	Probable-laboratory-supported	Limb	Right	Mild
2	43	M	6	Probable-laboratory-supported	Limb	Right	Mild
3	45	M	14	Probable-laboratory-supported	Limb	Left	Mild
4	52	M	26	Probable	Limb	Right	Severe
5	57	M	14	Definite	Bulbar	Right	Mild
						Left	Mild
6	57	M	13	Definite	Limb	Left	Severe
7	58	M	12	Probable	Limb	Left	Mild
8	59	F	6	Probable	Limb	Right	Moderate
9	59	F	3	Definite	Limb	Right	Mild
						Left	Mild
10	60	F	9	Probable	Bulbar	Right	Mild
						Left	Mild
11	62	M	11	Probable	Limb	Left	Mild
						Right	Mild
12	63	F	20	Definite	Limb	Left	Mild
13	64	M	35	Definite	Bulbar	Right	Mild
14	64	M	36	Definite	Limb	Right	Severe
15	64	F	6	Definite	Bulbar	Right	Mild
						Left	Moderate
16	64	F	3	Definite	Limb	Right	Mild
17	66	M	48	Probable-laboratory-supported	Limb	Left	Mild
18	68	M	24	Definite	Limb	Right	Mild
						Left	Moderate
19	68	F	72	Definite	Limb	Right	Mild
						Left	Mild
20	69	M	10	Definite	Limb	Right	Severe
						Left	Severe
21	70	F	10	Definite	Bulbar	Right	Moderate
22	71	F	10	Probable-laboratory-supported	Limb	Right	Mild
						Left	Severe
23	72	F	11	Definite	Bulbar	Right	Mild
						Left	Mild
24	73	M	8	Definite	Limb	Right	Moderate
25	74	M	4	Definite	Limb	Left	Moderate
26	79	M	24	Probable-laboratory-supported	Limb	Left	Mild

Fifteen healthy, age matched, volunteers were also studied. They all were free from neurological or other diseases and their ages ranged from 41 to 83 years (60.9 ± 12.4 years).

The purpose of the study was explained to every subject, and the informed consent to participation in the study was obtained from all the subjects. The study was approved by the Ethics Committee of the University of Tokyo.

In the patients, the right median nerve was stimulated in nine subjects, left in seven, and both in 10 (Table 1). In total, 36 SEPs were obtained from 26 patients. In the 15 healthy volunteers, the right median nerve was stimulated in 10 and both in five, and 20 SEPs were recorded in total. Because the amplitudes and latencies of every SEP component did not differ significantly between two sides ($P > 0.1$, unpaired Student's t-test), normal values were made from all the results obtained from both sides.

To see the clinico-physiological correlations, the strength of a median nerve innervated abductor pollicis brevis (APB) muscle at the stimulated side was assessed at the time of examination in ALS patients by manual muscle testing using the Medical Research Council (MRC) scale (scores from 0 to 5). The studied limbs were divided into three groups according to the muscle strength of APB: muscle strength of MRC 5-4 (defined as mild weakness group), MRC 3 (moderate), and MRC 2-0 (severe). In the 36 limbs, 24 APB muscles had mild weakness (MRC 5-4), 6 moderate (MRC 3), and 6 severe (MRC 2-0) (Table 2). In these patients, the level of weakness correlated with the degree of recruitment reduction in needle electromyographic studies of APB. There were no significant differences in age and body height among the four groups (mild, moderate, severe weakness and control) (age: [$F(3, 52) = 0.636$, $P = 0.595$]; body height: [$F(3, 52) = 0.516$, $P = 0.674$]) and in duration of the illness among the three groups ([$F(2, 33)$=0.681, $P = 0.513$]) (Table 2).

2.2. Data recordings

Somatosensory evoked potentials (SEPs) were elicited after electrical stimulation of the median nerve at the wrist using a constant current square wave pulse (0.2 ms duration). The anode was placed over the median nerve at the wrist, and the cathode 2.5 cm proximal to the anode. The stimulus intensity was about 4 times sensory threshold which was almost equivalent to 1.5 times motor threshold. The stimuli were delivered at a repetition rate of 2–3 Hz. Since the alertness has a profound influence on the HFOs (Emerson et al., 1988; Gobbelé et al., 2000; Yamada et al., 1988), we kept the subjects awake during the experiments. The alertness was monitored by EEG recordings from a midfrontal electrode (Fz) of the international 10-20 system with ear (A1) reference. For SEPs, recording electrodes were placed at two locations: the spinous process of C6 (CV 6), and C3′ or C4′ (2 cm posterior to the C3 (C4) of the international 10-20 system), with Fz reference. To confirm that stimuli activated peripheral nerves adequately in the experiments, the electrode was placed on the ipsilateral Erb's point for recording the N9 potential. The electrode impedances were kept less than 5 kΩ. Responses were amplified with filters set at 20 and 3000 Hz. 1000–2000 responses were averaged and then digitized with an analogue to digital converter at a sampling rate of 20 kHz. An epoch of 50 ms duration was obtained. At least two averaged responses were obtained under the same conditions to ascertain the reproducibility of SEPs.

We used C3′ (C4′)-Fz montage for recording HFOs because it is the best montage for recording oscillation potentials clearly (Curio et al., 1994; Hashimoto et al., 1996; Mochizuki et al., 1999). The oscillation potentials were obtained by digitally filtering raw SEPs from 500 to

Table 2
Main clinical characters and mean (±SD) latencies of SEP and number of HFOs for different groups of subjects

Group of subjects (Number of limbs)	Control ($N = 20$)	ALS total ($N = 36$)	Mild ($N = 24$)	Moderate ($N = 6$)	Severe ($N = 6$)
Age (years)	63.1 ± 12.8	62.9 ± 9.2	61.4 ± 10.0	68.0 ± 5.7	63.7 ± 7.6
Body height (cm)	156.8 ± 7.9	159.1 ± 6.7	158.9 ± 7.0	156.6 ± 2.9	160.8 ± 7.7
Disease duration (months)	–	17.0 ± 16.9	18.7 ± 19.4	9.7 ± 7.3	17.5 ± 11.0
Latency					
N13 onset (ms)	11.7 ± 0.5	11.5 ± 0.7	11.4 ± 0.8	11.9 ± 0.5	11.8 ± 0.6
N13 peak (ms)	12.7 ± 0.4	12.5 ± 0.7	12.4 ± 0.8	13.2 ± 0.4	12.7 ± 0.5
N20 onset (ms)	15.7 ± 0.7	15.5 ± 0.8	15.5 ± 0.8	15.8 ± 0.6	15.4 ± 1.1
N20 peak (ms)	18.8 ± 0.7	19.2 ± 0.9	19.1 ± 0.9	19.6 ± 1.5	19.2 ± 0.4
P25 peak (ms)	23.2 ± 2.0	24.9 ± 1.7*	25.1 ± 1.4*	24.9 ± 1.9	24.2 ± 2.5
N20 onset–N20 peak (ms)	3.0 ± 0.7	3.6 ± 0.7*	3.6 ± 0.6	3.7 ± 0.8	3.9 ± 1.0
N13 peak–N20 peak (CCT) (ms)	6.1 ± 0.7	6.6 ± 0.7*	6.5 ± 0.7	7.1 ± 0.7	6.7 ± 0.3
N13 onset–N20 onset (ms)	4.1 ± 0.5	4.0 ± 0.5	4.0 ± 0.5	4.2 ± 0.5	4.4 ± 0.3
HFO: Number of peaks					
Onset–N20 peak	2.4 ± 0.5	2.4 ± 0.4	2.2 ± 0.4	2.5 ± 0.5	2.2 ± 0.4
Later than N20 peak	3.2 ± 0.7	2.9 ± 0.7	2.9 ± 0.7	3.5 ± 0.5	2.7 ± 0.5
CMAP (APB) (mV)	13.9 ± 2.6	6.9 ± 5.0*	9.5 ± 4.1**	6.5 ± 3.4**	0.7 ± 0.7**

Age, body height and SEP latencies of 15 control subjects and 24 ALS patients. "N" indicates number of studied limbs. 20 limbs from normal subjects and 36 limbs from the patients.
Asterisk indicates significant difference from the control data (*$P < 0.05$, **$P < 0.01$).

1000 Hz (Butterworth type, 12 dB/octave), using a Neuropack Micro computer system (Nihon Kohden, Japan).

In wide-band SEPs, onset latencies of N13 (N13o) and N20 (N20o), peak latencies of N13 (N13p), N20 (N20p) and P25 (P25p) components were measured. Sonoo et al. (1996) reported that the N13 (they named N13′ to distinguish from the components recorded with a non-cephalic reference) onset in the CV6-Fz lead nearly coincided with the P13/14 onset. The origin of P13/14 is thought to be localized at a small region around foramen magnum and cuneate nucleus, whereas the N13 onset and P13/14 onset are not always coincident completely (Sonoo et al., 1996). On the basis of these facts, special attention must be needed to evaluate latencies. Therefore, we measured the interval between the onsets of N13 and N20 (N13o–N20o), which may represent conduction from a site around the foramen magnum to the sensory cortex, to evaluate the intracranial sensory conduction. We also measured an interval between N13 peak and N20 peak (N13p–N20p) which was conventionally called the central sensory conduction time (CCT). We measured amplitudes of N20 onset-peak (N20o–N20p) and N20 peak-P25 peak (N20p–P25p) in wideband recordings.

For identification of HFOs, we used the same method as that described by Hashimoto and colleagues (Nakano and Hashimoto, 1999, 2000; Inoue et al., 2004). The oscillations after the onset of primary cortical response (N20) with an amplitude of twice or larger than that of background noises were considered as components of HFOs. The noise level was measured between 8 and 14 ms after the stimulus. Because early and late HFOs are considered to be generated by different mechanisms (Haueisen et al., 2000; Klostermann et al., 1999, 2000; Mochizuki et al., 1999; Nakano and Hashimoto, 1999), we analyzed two parts of HFOs separately: the early HFOs (HFOs from the onset to peak of N20) and the late HFOs (HFOs later than the N20 peak). The HFO whose peak was identical to the N20 peak was treated as a component of early HFOs (Inoue et al., 2004). We calculated the average amplitude of the early and late HFOs and compared these values between the patients and normal subjects. The amplitude ratios of early or late HFOs to the N20o–N20p were used to evaluate relations between SEP main components and HFOs. We also counted the number of negative peaks of HFOs within early and late parts.

We also recorded compound muscle action potentials (CMAPs) from APB and measured their sizes. Their relation to the muscle strength assessed by the MRC scale (de Carvalho and Swash, 2000) was also evaluated. CMAP was recorded with surface Ag/AgCl electrodes: an active electrode placed over the muscle belly and a reference electrode over the tendon. A ground electrode was placed between the wrist and the recording electrode. A conventional bipolar electrical stimulation (0.2 ms duration, cathode distal) was applied to the median nerve at 3 cm proximal to the distal crease of the wrist. Supramaximal stimulation was ensured by increasing the stimulus intensity until no further enlargement was obtained in CMAPs (Kimura, 2001). Usually, we recorded CMAPs elicited at intensity 1.3 times the minimal intensity to elicit maximal CMAPs. Responses were amplified with filters set at 2 Hz and 3 kHz. Sampling rate was 20 kHz. The peak to peak amplitude was measured.

2.3. Data analysis

We compared latencies (N13o, N13p, N20o, N20p, P25p, N13o–N20o, N20o–N20p, and N13p–N20p) and the numbers of HFOs peaks at each part between the patients and healthy volunteers using unpaired Student's *t*-test. We also compared those latencies, amplitudes (CMAP, N20o–N20p and N20p–P25p) and the numbers of HFOs peaks among four groups (control, mild, moderate, and severe weakness) using one way analysis of variance (ANOVA), and post hoc comparisons were made with Bonferroni method to compensate for multiple comparisons. P values less than 0.05 after compensation for multiple comparisons were considered to be significant.

3. Results

In all examined subjects, SEPs and HFOs were recorded clearly.

3.1. SEP amplitudes, HFO amplitudes and number of HFOs peaks

Typical SEPs and HFOs of patients with different levels of weakness are shown in Fig. 1. Two SEPs are superimposed in every trace. In the patient with moderate weakness (case 18), the N20 was larger than that of the patient with mild weakness (case 12). In the patient with severe weakness (case 6), the N20 was abnormally small though the amplitudes of N9 and N13 were normal (Fig. 1c). The amplitudes of early and late HFOs were in parallel with those of main components of SEP (Fig. 1b).

The N20o–N20p and N20p–P25p amplitudes of all subjects were sorted by the levels of weakness and plotted (Fig. 2). One way ANOVA revealed that the group of subjects had a significant effect on both N20o–N20p [$F(3,52) = 10.904$. $P < 0.001$] and N20p–P25p amplitudes [$F(3,52) = 11.368$. $P < 0.001$]. Post hoc analysis revealed following differences. The N20o–N20p amplitude of moderate weakness group (mean ± SD; 5.40 ± 1.81 μV) was significantly larger than those of healthy control (2.38 ± 1.11; $P < 0.001$), mild (3.45 ± 1.50; $P = 0.018$) and severe weakness groups (1.43 ± 1.17; $P < 0.001$). The N20p–P25p amplitude of moderate weakness group (9.92 ± 2.44) was significantly larger than that of control (4.60 ± 1.64; $P = 0.001$). Its amplitude of severe weakness group (1.76 ± 1.74) was significantly smaller than that of mild (6.80 ± 3.54; $P = 0.001$) or moderate weakness group ($P < 0.001$), whereas it was not significantly smaller than the size of healthy subjects ($P > 0.1$).

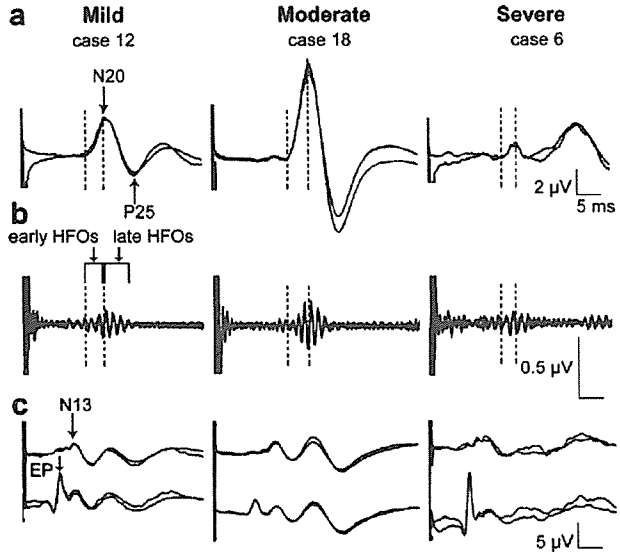

Fig. 1. Representative SEPs and HFOs in patients with different levels of weakness. Dotted line indicates the onset of N20. (a) N20 potential recorded from C3′ (C4′) to Fz montage. Note the amplitude of N20 markedly larger in the patient with moderate weakness (case 18) as compared with mild weakness patient (case 12). With severe weakness (case 6), a considerable decrease of the amplitude of N20 was observed. (b) HFOs obtained by digitally filtering raw SEPs from 500 to 1000 Hz. The amplitudes of early and late HFOs tend to be larger in a patient with moderate weakness than those with mild or severe weakness (c) Raw SEPs recorded from CV6-Fz and EP-Fz montage. Sufficient N9 and N13 potentials were evoked in all recordings.

For early HFOs (Fig. 3a, left), the group of subjects had a significant effect on their amplitude [$F(3,52) = 3.985$. $P = 0.013$]. The mean amplitudes were 0.15 ± 0.09 μV for healthy subjects, 0.19 ± 0.13 for mild, 0.28 ± 0.11 for moderate and 0.08 ± 0.05 for severe weakness groups. The amplitude of moderate weakness group was significantly larger than that of severe weakness group ($P = 0.013$). Although the difference was not significant ($P > 0.1$), the early HFOs changed in size in parallel with the size changes of main components of SEP in ALS. On the other hand, the amplitude of late HFOs (Fig. 3a, right) was not significantly affected by the group of subjects [$F(3,52) = 1.167$. $P = 0.331$] (control, 0.22 ± 0.14; mild, 0.23 ± 0.18; moderate 0.27 ± 0.12; severe, 0.11 ± 0.10). To evaluate relation between SEP main components and HFOs, the size ratios of oscillations to N20o–N20p amplitude are shown in Fig. 3b. There were no significant differences in these values among four groups ($P > 0.05$). This indicates that HFO amplitudes changed proportionally to the changes in main component amplitudes of SEP.

The numbers of HFO peaks at each part are listed in Table 2. There were no significant differences between healthy subjects and ALS patients ($P > 0.1$, unpaired Student's t-test). The group of subjects did not significantly affect the number of HFOs peaks at each part (onset–N20 peak; $F(3,52) = 1.760$, $P > 0.1$, later than N20 peak; $F(3,52) = 2.319$, $P > 0.05$).

3.2. SEP latencies

The latencies of P25p, N20o–N20p (duration of N20), and N13p–N20p (conventional CCT) of ALS patients (Table 2) were significantly longer than those of healthy subjects ($P < 0.05$, unpaired Student's t-test). The latencies of N13o, N20o, N13p, N20p, and N13o–N20o did not significantly differ between two groups. The group of subjects had a significant effect on P25p latency [$F(3,52) = 3.218$, $P = 0.032$]. The latency of mild weakness group was significantly longer than that of normal subjects ($P = 0.030$). The group of subjects did not affect the remaining latencies ($P > 0.05$).

3.3. CMAP amplitudes in APB

One way ANOVA revealed that the group of subjects had a significant effect on CMAP [$F(3,52) = 22.944$. $P < 0.001$]. The CMAP of control group was significantly larger than those of mild ($P < 0.001$), moderate ($P < 0.001$) and severe weakness groups ($P < 0.001$) (Table

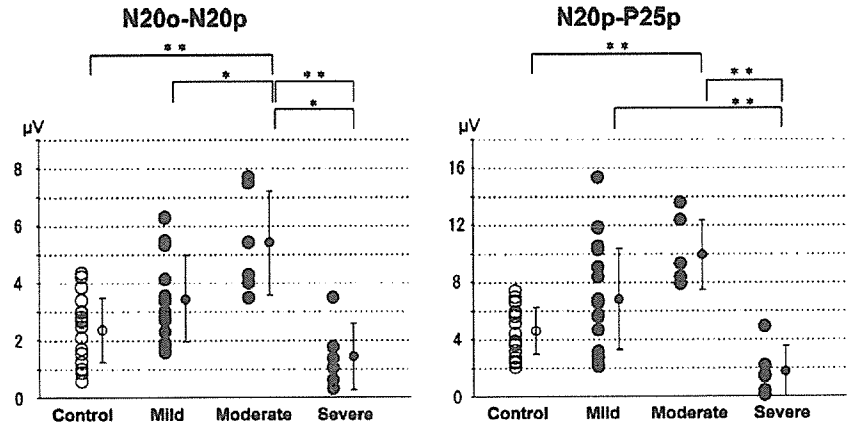

Fig. 2. Plots of the amplitudes of N20o–N20p (left) and N20p–P25p (right) components against the level of weakness. Circles indicate control subjects and dots ALS patients. Error bars indicate standard deviations. $^{*}P < 0.05$, $^{**}P < 0.01$.

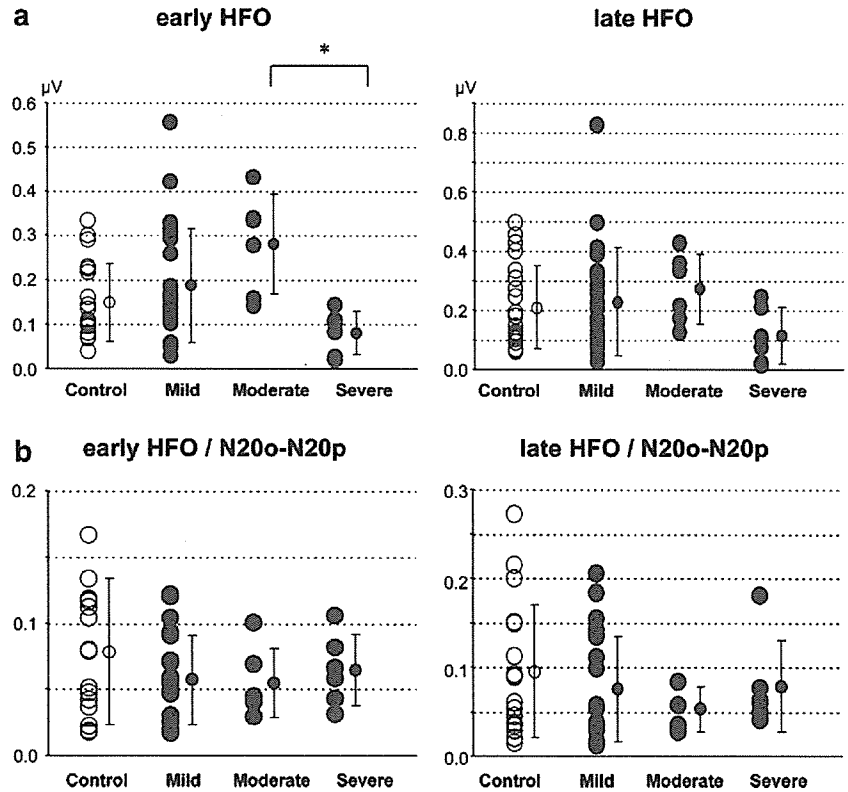

Fig. 3. (a) Plots of the amplitudes of early (left) and late (right) HFOs against the level of weakness. (b) Plots of the size ratio of HFOs to main component of SEP. $^{*}P < 0.05$.

2). There was also significant difference between mild and severe weakness groups ($P < 0.001$).

4. Discussion

We report three new findings. First, the amplitudes of N20o–N20p and N20p–P25p were abnormally enlarged in ALS patients with moderate weakness, while they attenuated in those with severe weakness. This was not due to insufficient peripheral stimulation because normal N9 potentials were elicited in all the patients. Second, both the early and late HFOs changed in size in parallel with the size changes of main components of SEP in ALS. The association between the main components and HFOs was confirmed by the constant size ratios of HFOs to the main component of SEP irrespective of the level of weakness. Finally, in ALS, the N13p–N20p conduction time (conventional CCT), N20o–N20p (duration of N20) and P25p latency were prolonged without any other latency abnormalities. Our present investigation is the first report about HFOs in ALS, and none of previous studies reported an enlargement of the N20 potential in ALS.

The N20 component of median nerve SEP is considered to reflect initial excitation of neurons in area 3b (Allison et al., 1991; Tiihonen et al., 1989). In contrast, even though several candidates have been proposed as a generator of HFOs, such as brainstem, thalamus, thalamocortical presynaptic action potentials and somatosensory cortex (Curio et al., 1997; Eisen et al., 1984; Gobbelé et al., 1998, 2004; Hashimoto et al., 1996, 1999; Klostermann et al., 2002; Shimazu et al., 2000), their generators remain to be determined (see a review by Mochizuki and Ugawa, 2005). The seminal work by Hashimoto et al. (1996) revealed the dissociation between SEP and HFOs amplitudes during a wake–sleep cycle. Thus, they proposed that HFOs reflect activities of inhibitory interneurons which are strongly associated with excitatory postsynaptic potentials (N20 amplitude) through feed forward and feed back inhibitions (Hashimoto et al., 1996; Nakano and Hashimoto, 1999; Tanosaki et al., 2002).

4.1. Amplitude changes in the N20 component

On the basis of the above notions, there are at least three possibilities to explain the SEP amplitude changes here reported in ALS.

(1) In humans, several studies using transcranial magnetic stimulation (TMS) indicate that pure sensory input can facilitate motor cortex (M1) (Hamdy et al., 1998; Kaelin-Lang et al., 2002; Ridding et al., 2000; Rosenkranz and Rothwell, 2003, 2004; Terao et al., 1995, 1999). These reports indicate there must be some mechanisms by which the sensory system mod-

ulates the motor cortical excitability. Corticocortical connections between areas 3a, 4 and 3b are present and topographically organized (Burton and Fabri, 1995; De Felipe et al., 1986; Krubitzer and Kaas, 1990). Thus, as well as subcortical structures, the sensory cortex might directly modulate the motor cortex. This sensory cortical driving of M1 may be enhanced to compensate for the affected motor cortex in ALS. This leads to the sensory cortical hyperexcitability, which is recognized as an enlargement of N20 potential in patients with moderate weakness. Then, small N20 in patients with severe weakness suggests that the compensation is no longer effective in those patients.

In ALS, the patients may need some mechanisms to compensate their weakness for precise and purposeful movements. One functional magnetic resonance imaging study suggested that cortical reorganization between motor related areas was a kind of partial compensation to optimize motor performances in ALS (Konrad et al., 2002). Some kind of compensatory function by non-motor system must exist in ALS patients. We speculate compensatory changes for motor dysfunction might occur not only in motor related areas but also in the somatosensory system. To use a weakened hand effectively, the patients may use sensory information much more powerfully than healthy subjects when they had moderate weakness, and these compensatory functions may disappear when the disease progresses because it becomes impossible to move their hands even with much compensation.

(2) The efferent signals from the motor cortex elicited by intracortical microstimulation diminished the size of any components of SEP generated by the sensory cortex in the monkey (Jiang et al., 1990). To date, various gating studies have confirmed that an early cortical response (N20) is attenuated by motor interferences (Gobbelé et al., 2003; Kakigi et al., 1995; Mochizuki et al., 2004; Rossini et al., 1999; Tanosaki et al., 2002; Valeriani et al., 1999). Though the precise mechanism is still a matter of controversy, one plausible explanation for this phenomenon is centrifugal gating hypothesis (Cohen and Starr, 1987). Attenuation of SEPs can be carried out by inhibitory interaction between the sensory signals and the efferent signals from motor related areas. Thus, in ALS patients, motor system disturbances may reduce inhibition of the sensory cortex, which finally leads to an enlargement of N20 potential. This possibility is unlike because SEPs were not enhanced but diminished in patients with severe weakness. If the above explanation is the case, SEPs would be more enhanced in the group of severe weakness.

Another possible influence on area 3b pyramidal cells by motor tasks is based on the intense cortico-cortical connections between area 3a and 3b (Kaas and Pons, 1988). Area 3a, which receives afferent signals from the muscles and joints, may reduce SEP sizes. This mechanism is called centripetal gating (Jones et al., 1989). We speculate the sensory input from muscle spindle must decrease in ALS because of inability of stretching spindles. This less gating of sensory cortex must enlarge the cortical potentials of SEP. This hypothesis also cannot explain the fact that SEPs were diminished in the patients with severe weakness.

(3) Neuropathological involvement of non-motor systems is well recognized in ALS patients. Neuronal loss may be seen in subcortical structures, including the basal ganglia, locus ceruleus, substantia nigra, thalamus, and so on (Lowe and Leigh, 2002). Based on the pathologically proven widespread involvement in ALS, one possible explanation for the N20/P25 changes is as follows: slight to moderate neuronal loss and gliosis were detected in the thalamic nuclei except for pulvinar thalamus in sporadic ALS patients who survived much longer with a respiratory support (Hayashi and Kato, 1989). It seems likely that some excitability changes occur in those thalamic nuclei in the late stage ALS. If the inhibitory reticular thalamic nucleus is involved, the N20 potential must be enhanced. If this is the case, SEPs must be enlarged even at the late stage of the ALS, which is inconsistent with our results.

Another possible explanation based on widespread involvement of extramotor systems is as follows. Some TMS studies revealed the lower motor threshold in the early stage of the ALS (Eisen et al., 1993; Mills and Nithi, 1997), and the others revealed abnormal firing patterns in the peristimulus time histograms in ALS (Eisen et al., 1996; Kohara et al., 1996; Mills, 1995). These results suggested the corticomotor hyperexcitability. This hyperexcitability is considered to be due to monoamine neuroexcitotoxicity in ALS. Therefore, we can speculate that similar neuroexcitotoxic changes occur in the sensory cortex, one of extramotor systems, which must cause SEP enlargements. Further studies are needed to determine whether it is the case in ALS.

4.2. Amplitude changes in the HFOs

The results showed that the early and late HFOs tended to be enlarged in patients with moderate weakness. The HFO/N20 amplitude ratios were not affected by the degree of weakness.

According to the hypothesis proposed by Hashimoto and coworkers, HFOs must reflect activities of inhibitory interneurons activated by both thalamocortical afferents and excitatory synaptic inputs from pyramidal neurons of area 3b through their local axon collaterals (Hashimoto et al., 1996; Nakano and Hashimoto, 1999; Tanosaki et al., 2002). If so, they reflect both feed forward and feed

back inhibitory effects onto the post synaptic pyramidal neurons of the sensory cortex. They claimed that one function of inhibitory interneurons of the sensory cortex must be a stabilization of the pyramidal cell activity, similar to that of Renshow cell in the spinal cord (Tanosaki et al., 2002). Based on this hypothesis, we can speculate that, in ALS patients with moderate weakness, the compensatory hyperexcitable sensory cortex may be stabilized by inhibitory interneurons comparably active to the hyperexcitable pyramidal neurons. In patients with severe weakness, inhibitory interneurons may not be activated because of the low activity of excitatory sensory pyramidal neurons. Such modulation from the pyramidal neurons toward the interneurons can explain the parallel behavior of HFO and N20/P25 potential and also explain some previous results which show the absence of a dissociation between HFOs and main components of SEP in aged or young healthy subjects and in patients with myoclonus epilepsy (Mochizuki et al., 1999; Nakano and Hashimoto, 1999, 2000). Another possibility to explain our results is that HFOs do not purely reflect the inhibitory interneuron activities and the dissociation between HFOs and SEP components is not a universal phenomenon.

4.3. Sensory conduction time in ALS

Many studies of SEP in ALS are conflicting: some reports revealed no SEP abnormalities (Cascino et al., 1988; Chiappa, 1983; Oh et al., 1985), while others showed conduction delays in upper limb SEPs (Bosch et al., 1985; Cosi et al., 1984; Dasheiff et al., 1985; Radtke et al., 1986; Subramaniam and Yiannikas, 1990; Theys et al., 1999; Zanette et al., 1990) and lower limb SEPs (Georgesco et al., 1997; Matheson et al., 1986; Radtke et al., 1986; Subramaniam and Yiannikas, 1990; Zanette et al., 1996). They were delays of N13–N19 (Bosch et al., 1985; Cosi et al., 1984; Subramaniam and Yiannikas, 1990; Zanette et al., 1990) and N9–N20 interpeak latencies (Radtke et al., 1986; Theys et al., 1999). The prolonged conventional CCT in our results is consistent with such previous studies. However, we should interpret these results carefully. The interpeak latency of N13–N20 is widely accepted as "central sensory conduction time" even though various issues concerning them remain to be investigated (Sonoo et al., 1996; Tanosaki et al., 1999). Because the amplitude of N20 positively correlated with its duration (Sonoo et al., 1997), alternation of the N20 amplitude may cause changes in the conventional CCT. In ALS, the enhanced N20 must cause prolongation of the conventional CCT and duration of N20. In addition, no differences were found in any other latency parameters between ALS and healthy subjects; the onset latency of N13 and N20, the interval of N13o–N20o and the peak latency of N13 and N20. These suggest that the intracranial sensory conduction was not prolonged in ALS. Based on these, we conclude that in ALS, the prolonged conventional CCT is not due to a conduction delay in the central sensory system but due to a prolongation of N20 production processes.

Based on the above arguments, we have two conclusions. (1) The amplitude alternation of N20 potential has some relation with the severity of weakness. Enlarged N20 potential must reflect somatosensory compensation for motor system dysfunction in ALS. (2) In ALS patients, the prolonged conventional CCT does not indicate a conduction delay in the sensory system, but it suggests an alternation of some central sensory processing.

Acknowledgements

Part of this work was supported by Research Project Grant-in-aid for Scientific Research No. 17590865 (RH), No. 18590928 (YT), No. 16500194 (YU) from the Ministry of Education, Science, Sports and Culture of Japan, grants for the Research Committee on rTMS treatment of movement disorders, the Ministry of Health and Welfare of Japan (17231401), the Research Committee on dystonia, the Ministry of Health and Welfare of Japan, a grant from the Committee of the Study of Human Exposure to EMF, Ministry of Public Management, Home Affairs, Post and Telecommunications.

References

Allison T, McCarthy G, Wood CC, Jones SJ. Potentials evoked in human and monkey cerebral cortex by stimulation of the median nerve. A review of scalp and intracranial recordings. Brain 1991;114:2465–503.

Bosch EP, Yamada T, Kimura J. Somatosensory evoked potentials in motor neuron disease. Muscle Nerve 1985;8:556–62.

Brooks BR, Miller RG, Swash M, Munsat TL. World Federation of Neurology Research Group on Motor Neuron Diseases. El Escorial revisited: revised criteria for the diagnosis of amyotrophic lateral sclerosis. Amyotroph Lateral Scler Other Motor Neuron Disord 2000;1:293–9.

Burton H, Fabri M. Ipsilateral intracortical connections of physiologically defined cutaneous representations in areas 3b and 1 of macaque monkeys: projections in the vicinity of the central sulcus. J Comp Neurol 1995;355:508–38.

Cascino GD, Ring SR, King PJ, Brown RH, Chiappa KH. Evoked potentials in motor system diseases. Neurology 1988;38:231–8.

Chiappa KH. Evoked potentials in clinical medicine. New York: Raven Press; 1983.

Cohen LG, Starr A. Localization, timing and specificity of gating of somatosensory evoked potentials during active movement in man. Brain 1987;110:451–67.

Cosi V, Poloni M, Mazzini L, Callieco R. Somatosensory evoked potentials in amyotrophic lateral sclerosis. J Neurol Neurosurg Psychiatry 1984;47:857–61.

Curio G, Marckert BM, Burghoff M, Koetitz R, Abraham-Fuchs K, Härer W. Localization of evoked neuromagnetic 600 Hz activity in the cerebral somatosensory system. Electroenceph Clin Neurophysiol 1994;91:483–7.

Curio G, Mackert BM, Burghoff M, Neumann J, Nolte G, Scherg M, et al. Somatotopic source arrangement of 600 Hz oscillatory magnetic fields at the human primary somatosensory hand cortex. Neurosci Lett 1997;234:131–4.

Dasheiff RM, Drake ME, Brendle A, Erwin CW. Abnormal somatosensory evoked potentials in amyotrophic lateral sclerosis. Electroenceph Clin Neurophysiol 1985;60:306–11.

de Carvalho M, Swash M. Nerve conduction studies in amyotrophic lateral sclerosis. Muscle Nerve 2000;23:344–52.

De Felipe J, Conley M, Jones EG. Long-range focal collateralization of axons arising from corticocortical cells in monkey sensory-motor cortex. J Neurosci 1986;6:3749–66.

Eisen A, Roberts K, Low M, Hoirch M, Lawrence P. Questions regarding the sequential neural generator theory of the somatosensory evoked potential raised by digital filtering. Electroenceph Clin Neurophysiol 1984;59:388–95.

Eisen A, Pant B, Stewart H. Cortical excitability in amyotrophic lateral sclerosis: a clue to pathogenesis. Can J Neurol Sci 1993;20:11–6.

Eisen A, Entezari Taher M, Stewart H. Cortical projections to spinal motoneurons: changes with aging and amyotrophic lateral sclerosis. Neurology 1996;46:1396–404.

Emerson RG, Sgro JA, Pedley TA, Hauser WA. State-dependent changes in the N20 component of the median nerve somatosensory evoked potential. Neurology 1988;38:64–8.

Georgesco M, Salerno A, Camu W. Somatosensory evoked potentials elicited by stimulation of lower-limb nerves in amyotrophic lateral sclerosis. Electroenceph Clin Neurophysiol 1997;104: 333–42.

Gobbelé R, Buchner H, Curio G. High-frequency (600 Hz) SEP activities originating in the subcortical and cortical human somatosensory system. Electroencephalogr Clin Neurophysiol 1998;108: 182–9.

Gobbelé R, Waberski TD, Kuelkens S, Sturm W, Curio G, Buchner H. Thalamic and cortical high-frequency (600 Hz) somatosensory-evoked potential (SEP) components are modulated by slight arousal changes in awake subjects. Exp Brain Res 2000;133:506–13.

Gobbelé R, Waberski TD, Thyerlei D, Thissen M, Darvas F, Klostermann F, et al. Functional dissociation of a subcortical and cortical component of high-frequency oscillations in human somatosensory evoked potentials by motor interference. Neurosci Lett 2003;350:97–100.

Gobbelé R, Waberski TD, Simon H, Peters E, Klostermann F, Curio G, et al. Different origins of low and high frequency components (600 Hz) of human somatosensory evoked potentials. Clin Neurophysiol 2004;115:927–37.

Hamdy S, Rothwell JC, Aziz Q, Singh KD, Thompson DG. Long-term reorganization of human motor cortex driven by short-term sensory stimulation. Nat Neurosci 1998;1:64–8.

Hashimoto I, Mashiko T, Imada T. Somatic evoked high-frequency magnetic oscillations reflect activity of inhibitory interneurons in the human somatosensory cortex. Electroenceph Clin Neurophysiol 1996;100:189–203.

Hashimoto I, Kimura T, Fukushima T, Iguchi Y, Saito Y, Terasaki O, et al. Reciprocal modulation of somatosensory evoked N20m primary response and high-frequency oscillations by interference stimulation. Clin Neurophysiol 1999;110:1445–51.

Haueisen J, Heuer T, Nowak H, Liepert J, Weiller C, Okada Y, et al. The influence of lorazepam on somatosensory-evoked fast frequency (600 Hz) activity in MEG. Brain Res 2000;874:10–4.

Hayashi H, Kato S. Total manifestations of amyotrophic lateral sclerosis. ALS in the totally locked-in state. J Neurol Sci 1989;93:19–35.

Inoue K, Hashimoto I, Shirai T, Kawakami H, Miyachi T, Mimori Y, et al. Disinhibition of the somatosensory cortex in cervical dystonia – decreased amplitudes of high frequency oscillations. Clin Neurophysiol 2004;115:1624–30.

Jiang W, Chapman CE, Lamarre Y. Modulation of somatosensory evoked responses in the primary somatosensory cortex produced by intracortical microstimulation of the motor cortex in the monkey. Exp Brain Res 1990;80:333–44.

Jones SJ, Halonen JP, Shawkat F. Centrifugal and centripetal mechanisms involved in the 'gating' of cortical SEPs during movement. Electroenceph Clin Neurophysiol 1989;74:36–45.

Kaas JH, Pons TP. The somatosensory system in primates. Comp Primate Biol 1988;4:421–68.

Kaelin-Lang A, Luft AR, Sawaki L, Burstein AH, Sohn YH, Cohen LG. Modulation of human corticomotor excitability by somatosensory input. J Physiol 2002;540:623–33.

Kakigi R, Koyama S, Hoshiyama M, Watanabe S, Shimojo M, Kitamura Y. Gating of somatosensory evoked responses during active finger movements magnetoencephalographic studies. J Neurol Sci 1995;128:195–204.

Kimura J. Electrodiagnosis in diseases of nerve and muscle: principles and practice. 3rd ed. New York, NY: Oxford University Press; 2001.

Klostermann F, Nolte G, Curio G. Multiple generators of 600 Hz wavelets in human SEP unmasked by varying stimulus rates. Neuroreport 1999;10:1625–9.

Klostermann F, Funk T, Vesper J, Siedenberg R, Curio G. Double-pulse stimulation dissociates intrathalamic and cortical high-frequency (>400 Hz) SEP components in man. Neuroreport 2000;11:1295–9.

Klostermann F, Gobbelé R, Buchner H, Curio G. Intrathalamic non-propagating generators of high-frequency (1000 Hz) somatosensory evoked potential (SEP) bursts recorded subcortically in man. Clin Neurophysiol 2002;113:1001–5.

Kohara N, Kaji R, Kojima Y, Mills KR, Fujii H, Hamano T, et al. Abnormal excitability of the corticospinal pathway in patients with amyotrophic lateral sclerosis: a single motor unit study using transcranial magnetic stimulation. Electroenceph Clin Neurophsiol 1996;101:32–41.

Konrad C, Henningsen H, Bremer J, Mock B, Deppe M, Buchinger C, et al. Pattern of cortical reorganization in amyotrophic lateral sclerosis: a functional magnetic resonance imaging study. Exp Brain Res 2002;143:51–6.

Krubitzer LA, Kaas JH. The organization and connections of somatosensory cortex in marmosets. J Neurosci 1990;10:952–74.

Lowe JS, Leigh N. Disorders of movement and system degenerations. In: Graham DI, Lantos PL, editors. Greenfield's neuropathology. 7th ed. New York, NY: Oxford University Press; 2002. p. 372–83.

Matheson JK, Harrington HJ, Hallett M. Abnormalities of multimodality evoked potentials in amyotrophic lateral sclerosis. Arch Neurol 1986;43:338–40.

Mills KR. Motor neuron disease. Studies of the corticospinal excitation of single motor neurons by magnetic brain stimulation. Brain 1995;118:971–82.

Mills KR, Nithi K. Corticomotor threshold is reduced in early idiopathic amyotrophic lateral sclerosis. Muscle Nerve 1997;20:1137–41.

Mochizuki H, Ugawa Y. High-frequency oscillations in somatosensory system. Clin EEG Neurosci 2005;36:278–84.

Mochizuki H, Ugawa Y, Machii K, Terao Y, Hanajima R, Furubayashi T, et al. Somatosensory evoked high-frequency oscillation in Parkinson's disease and myoclonus epilepsy. Clin Neurophysiol 1999;110:185–91.

Mochizuki H, Terao Y, Okabe S, Furubayashi T, Arai N, Iwata NK, et al. Effects of motor cortical stimulation on the excitability of contralateral motor and sensory cortices. Exp Brain Res 2004;158:519–26.

Nakano S, Hashimoto I. The later part of high-frequency oscillations in human somatosensory evoked potentials is enhanced in aged subjects. Neurosci Lett 1999;276:83–6.

Nakano S, Hashimoto I. High-frequency oscillations in human somatosensory evoked potentials are enhanced in school children. Neurosci Lett 2000;291:113–6.

Oh SJ, Sunwoo IN, Kim HS, Faught E. Cervical and cortical somatosensory evoked potentials differentiate cervical spondylotic myelopathy from amyotrophic lateral sclerosis (abstract). Neurology 1985;35 suppl 1:147–8.

Radtke RA, Erwin A, Erwin CW. Abnormal sensory evoked potentials in amyotrophic lateral sclerosis. Neurology 1986;36:796–801.

Ridding MC, Brouwer B, Miles TS, Pitcher JB, Thompson PD. Changes in muscle responses to stimulation of the motor cortex induced by peripheral nerve stimulation in human subjects. Exp Brain Res 2000;131:135–43.

Rosenkranz K, Rothwell JC. Differential effect of muscle vibration on intracortical inhibitory circuits in humans. J Physiol 2003;551: 649–60.

Rosenkranz K, Rothwell JC. The effect of sensory input and attention on the sensorimotor organization of the hand area of the human motor cortex. J Physiol 2004;561:307–20.

Rossini PM, Babiloni C, Babiloni F, Ambrosini A, Onorati P, Carducci F, et al. "Gating" of human short-latency somatosensory evoked cortical responses during execution of movement. A high resolution electroencephalography study. Brain Res 1999;843:161–70.

Shimazu H, Kaji R, Tsujimoto T, Kohara N, Ikeda A, Kimura J, et al. High-frequency SEP components generated in the somatosensory cortex of the monkey. Neuroreport 2000;11:2821–6.

Sonoo M, Kobayashi M, Genba-Shimizu K, Mannen T, Shimizu T. Detailed analysis of the latencies of median nerve somatosensory evoked potential components, 1: selection of the best standard parameters and the establishment of normal values. Electroenceph Clin Neurophysiol 1996;100:319–31.

Sonoo M, Genba-Shimizu K, Mannen T, Shimizu T. Detailed analysis of the latencies of median nerve somatosensory evoked potential components, 2: analysis of subcomponents of the P13/14 and N20 potentials. Electroenceph Clin Neurophysiol 1997;104:296–311.

Subramaniam JS, Yiannikas C. Multimodality evoked potentials in motor neuron disease. Arch Neurol 1990;47:989–94.

Tanosaki M, Ozaki I, Shimamura H, Baba M, Matsunaga M. Effects of aging on central conduction in somatosensory evoked potentials: evaluation of onset versus peak methods. Clin Neurophysiol 1999;110:2094–103.

Tanosaki M, Kimura T, Takino R, Iguchi Y, Suzuki A, Kurobe Y, et al. Movement interference attenuates somatosensory high-frequency oscillations: contribution of local axon collaterals of 3b pyramidal neurons. Clin Neurophysiol 2002;113:993–1000.

Terao Y, Ugawa Y, Uesaka Y, Hanajima R, Gemba-Shimizu K, Ohki Y, et al. Input–output organization in the hand area of the human motor cortex. Electroenceph Clin Neurophysiol 1995;97:375–81.

Terao Y, Ugawa Y, Hanajima R, Furubayashi T, Machii K, Enomoto H, et al. Air-puff-induced facilitation of motor cortical excitability studied in patients with discrete brain lesions. Brain 1999;122:2259–77.

Theys PA, Peeters E, Robberecht W. Evolution of motor and sensory deficits in amyotrophic lateral sclerosis estimated by neurophysiological techniques. J Neurol 1999;246:438–42.

Tiihonen J, Hari R, Hämäläinen M. Early deflections of cerebral magnetic responses to median nerve stimulation. Electroenceph Clin Neurophysiol 1989;74:290–6.

Valeriani M, Restuccia D, Di Lazzaro V, Le Pera D, Tonali P. Effect of movement on dipolar source activities of somatosensory evoked potentials. Muscle Nerve 1999;22:1510–9.

Yamada T, Kameyama S, Fuchigami Y, Nakazumi Y, Dickins QS, Kimura J. Changes of short latency somatosensory evoked potential in sleep. Electroenceph Clin Neurophysiol 1988;70:126–36.

Zanette G, Polo A, Gasperini M, Bertolasi L, de Grandis D. Far-field and cortical somatosensory evoked potentials in motor neuron disease. Muscle Nerve 1990;13:47–55.

Zanette G, Tinazzi M, Polo A, Rizzuto N. Motor neuron disease with pyramidal tract dysfunction involves the cortical generators of the early somatosensory evoked potential to tibial nerve stimulation. Neurology 1996;47:932–8.

ELSEVIER

NeuroImage

www.elsevier.com/locate/ynimg
NeuroImage 31 (2006) 699 – 709

Effect of repetitive transcranial magnetic stimulation applied over the premotor cortex on somatosensory-evoked potentials and regional cerebral blood flow

Ryo Urushihara,[a,b] Nagako Murase,[a] John C. Rothwell,[c] Masafumi Harada,[d] Yuki Hosono,[a] Kotaro Asanuma,[a] Hideki Shimazu,[a] Kazumi Nakamura,[a] Sachiko Chikahisa,[b] Kazuyoshi Kitaoka,[b] Hiroyoshi Sei,[b] Yusuke Morita,[b] and Ryuji Kaji [a,*]

[a]*Department of Clinical Neuroscience, Institute of Health Biosciences, The University of Tokushima Graduate School, Kuramoto, Tokushima 770-8503, Japan*
[b]*Department of Integrative Physiology, Institute of Health Biosciences, The University of Tokushima Graduate School, Kuramoto, Tokushima 770-8503, Japan*
[c]*MRC Human Movement and Balance Unit, Institute of Neurology, Queen Square, London, UK*
[d]*Department of Radiologic Technology, School of Health Sciences, The University of Tokushima, Kuramoto, Tokushima 770-8509, Japan*

Received 18 September 2005; revised 25 November 2005; accepted 15 December 2005
Available online 8 February 2006

Somatosensory-evoked potentials (SEPs) are attenuated by movement. This phenomenon of 'gating' reflects sensorimotor integration for motor control. The frontal N30 component after median nerve stimulation was shown to be reduced in amplitude prior to hand movement. To investigate the mechanism of this sensory gating, we recorded median SEPs immediately before and after application of monophasic very low-frequency (0.2 Hz) repetitive transcranial magnetic stimulation (rTMS) of 250 stimuli over motor cortex (MC), premotor cortex (PMC), or supplementary motor area (SMA) in 9 healthy volunteers. The stimulus intensity for MC or PMC was set 85% of the resting motor threshold for the hand muscle, and that for SMA was at the active motor threshold for the leg muscle. SEPs showed significant increases in amplitudes of the frontal N30 component after PMC stimulation, but not after SMA or MC stimulation. Low-frequency (1 Hz) biphasic stimulation over PMC showed no significant N30 changes in 6 out of 9 subjects tested, indicating the effect being specific for 0.2 Hz monophasic stimulation. To examine the functional anatomy of the N30 change, single photon emission computed tomography was performed immediately before and after monophasic 0.2 Hz rTMS over PMC in all the 9 subjects. Regional cerebral blood flow showed significant increases mainly in PMC and prefrontal cortex, indicating the involvement of these cortical areas in sensory input gating for motor control.

Keywords: Somatosensory-evoked potential; Repetitive transcranial magnetic stimulation; Single photon emission computed tomography; Sensorimotor integration; Gating; N30

Introduction

Somatosensory-evoked potentials (SEPs) have been used to explore the central mechanism of sensory input processing. SEP amplitudes are attenuated during voluntary (Papakostopoulos et al., 1975; Cohen and Starr, 1987) and passive (Brooke et al., 1996) movement or under mental simulation of movement (Cheron and Borenstein, 1992; Rossi et al., 2002). This attenuation is referred to as "gating". SEPs are also gated before movement (Starr and Cohen, 1985; Shimazu et al., 1999; Asanuma et al., 2003), and clarification of its precise mechanism should help understand the sensorimotor integration in motor control of normal subjects and patients with basal ganglia disorders (Murase et al., 2000).

Transcranial magnetic stimulation (TMS) is a useful tool for studying the excitability and conductivity of the entire motor pathway from the cortex to the target muscle or the connectivity of the cerebral cortex. Recently, repetitive TMS (rTMS) has been used to apply a series of stimuli to a specific cortical area (Siebner and Rothwell, 2003; Murase et al., 2005). This can lead to long-lasting aftereffects on the excitability not only in the area itself, but also those areas that are functionally linked to it (Munchau et al., 2002). Because of its inhibitory effect on cortical excitability, low-frequency rTMS (<1 Hz) has been used for treating disorders related to brain hyperexcitability (Siebner et al., 1999; Hoffman and Cavus, 2002; Murase et al., 2005), whereas high-frequency rTMS (>5 Hz) exerts an excitatory influence on the cortex.

Non-primary motor areas may have an important role in sensorimotor integration for motor control because of their closer link to basal ganglia than the primary motor cortex. Although several studies have reported the effects of rTMS on SEPs (Enomoto et al., 2001; Tsuji and Rothwell, 2002; Satow et al., 2003; Ragert et al., 2004), only a few investigations have explored

* Corresponding author. Fax: +81 88 633 7208.
E-mail address: rkaji@clin.med.tokushima-u.ac.jp (R. Kaji).
Available online on ScienceDirect (www.sciencedirect.com).

1053-8119/$ - see front matter © 2005 Elsevier Inc. All rights reserved.
doi:10.1016/j.neuroimage.2005.12.027

the effect of rTMS applied over non-primary motor areas (Siebner et al., 2003; Murase et al., 2005). In this study, using the clinically effective stimulation parameters in writer's cramp (Murase et al., 2005), we recorded SEPs immediately before and after application of monophasic very low-frequency (0.2 Hz) rTMS over the primary and non-primary motor cortices of normal subjects to investigate the role of these areas on processing sensory input. In rTMS over PMC, we also recorded SEPs immediately before and after biphasic low-frequency (1 Hz) rTMS to investigate the frequency or phase specificity of the rTMS aftereffects on median SEPs. In addition, we recorded single photon emission computed tomography (SPECT) and compared regional cerebral blood flow (rCBF) images immediately before and after monophasic 0.2 Hz rTMS over PMC to investigate changes in cortical blood flow associated with those in SEPs.

Methods

Subjects

Nine healthy right-handed subjects (all men aged 30.2 ± 8.8 years) participated in this study. All subjects gave their informed consent for the study, which was approved by the Ethics Committee of the University of Tokushima, School of Medicine. The subjects were free from neurological and psychiatric diseases.

Experimental design

SEPs were recorded immediately before and after application of monophasic rTMS; 250 pulse trains were delivered at 0.2 Hz over the right-hand motor area (MC), the premotor area (PMC), or the supplementary motor area (SMA) in 9 subjects. To compare the effects of monophasic 0.2 Hz rTMS to the standard low-frequency rTMS used in many previous studies, we also recorded SEPs immediately before and after application of biphasic 1 Hz rTMS (250 pulse trains) over PMC in 6 of 9 subjects. The sessions were performed on separate days in a counterbalanced order at intervals of at least 1 week. In addition, we evaluated the effect of premotor monophasic very low-frequency rTMS on cortical blood flow using SPECT in the same 9 subjects who had SEP studies on separate days at least 1 week apart from the SEP recording session. In the present study, parameters of rTMS were in accordance with the international safety guidelines (Wassermann, 1998).

Recording and analysis of SEPs

In an electrically and auditory shielded room, the subjects sat comfortably on a reclining chair with their feet on the foot-rest and the neck supported by a U-shaped pillow to avoid head movement. SEPs were obtained by applying a 0.2-ms square electrical pulse at 1 Hz to the median nerve at the right wrist through a pair of surface electrodes. The intensity was adjusted just above the thumb twitch threshold. SEPs were recorded with silver chloride disk surface electrodes at F3 and C3′ (2 cm posterior to C3), according to the International 10–20 system. The linked earlobe electrodes served as the reference. The impedance of these electrodes was kept below 3 kΩ. The electrooculogram (EOG) was also recorded with a pair of silver chloride disk electrodes at 2 cm above and 2 cm below the right outer canthus. Signals from scalp electrodes and the EOG were amplified and acquired at a sampling rate of 10 kHz and filtered at 1–5000 Hz and 0.5–1000 Hz respectively (MEB2200 amplifier; Nihon Koden, Tokyo, Japan). All signals were recorded for 100 ms after the onset of median nerve stimulation and stored on a personal computer for off-line analysis. We collected at least 150 artifact-free sweeps and then averaged them off-line. To ensure SEP reproducibility, electrodes were left attached at the initial positions without being connected to the amplifier throughout the application of rTMS. Our preliminary studies confirmed that no current injury or electrode heating occurred after this procedure.

We identified 5 components at C3′, an initial positive peak with a latency of 10–16 ms (P14), a following negative large peak (N20), a second positive peak (P26), a second negative peak (N34) and a third positive peak (P45). For recordings from F3, 3 components following P14 were analyzed: a positive peak of 15–25 ms (P22) and two negative peaks (N30 and N60). We measured the base-to-peak amplitudes and the peak latencies of these components. The baseline was defined as the segment between 2 and 6 ms after stimulation.

In 2 of 9 subjects, we recorded median SEPs before and after application of monophasic 0.2 Hz rTMS over PMC with 62 scalp electrodes (a Ag/AgCl surface electrode cap system, Quickcap; Neuromedical Supplies Inc., El Paso, Texas, USA) to obtain SEP topographical mapping on the subject's real head model. Electrical stimulation was applied to the right median nerve as mentioned above. Signals were sampled at 5000 Hz and filtered at 1–1000 Hz (SynAmp amplifier and Scan software; Neuroscan Inc., El Paso, Texas, USA). We performed two recording sessions before and after application of rTMS, and about 200 sweeps were recorded in a single session. The data were stored in a personal computer and grand-averaged over 200 artifact-free sweeps for off-line analysis. With these waveforms, topographical maps of N30 components were calculated on a reconstructed realistic head model from their MRI images (Curry software; Neuroscan Inc., El Paso, Texas, USA).

rTMS

We used monophasic rTMS at 0.2 Hz over three sites (MC, PMC, SMA) by the same procedure in the previous clinical study with writer's cramp (Murase et al., 2005) and biphasic rTMS at 1 Hz only over PMC.

For stimulating MC on the left, a figure-of-eight stimulation coil (outside diameter of one half-coil, 8.7 cm) connected to a Magstim 200 stimulator (2.2 T at the coil surface when connected to the Magstim 200; Magstim Co. Ltd., OHR Wales, UK) was placed over the area 2 cm anterior and 3.5 cm lateral to Cz (International 10–20 System). The intensity of stimulation was increased from 30% of the maximum output of the stimulator in 5% steps until an MEP became just visible. The coil was then moved in 0.5-cm steps in all four directions, medially, laterally, posteriorly and anteriorly, until the maximum MEP was found on the right first dorsal interosseous muscle (hot spot). The stimuli were applied over the 'hot spot' with the figure-of-eight coil at a stimulus intensity set at 85% of the resting motor threshold (RMT).

The stimulation site for PMC was determined 2 cm anterior and 1 cm medial to the hot spot over the left hemisphere (Schluter et al., 1998). This was estimated from the dorsal premotor cortex established in a PET study (Fink et al., 1997). Stimuli were applied with the figure-of-eight coil, and the stimulus intensity was set at 85% of RMT for MC. We used the same coil and stimulator in MC session for monophasic 0.2 Hz stimulation. For biphasic 1 Hz

stimulation session, we used a figure-of-eight coil connected to Magstim rapid stimulator (Magstim Co. Ltd., OHR Wales, UK) to estimate RMT for MC and to deliver rTMS over PMC at 85% RMT using the same procedure as in monophasic stimulation.

The site for stimulating SMA was 2 cm anterior to the leg motor area (Muri et al., 1994; Fink et al., 1997). A double-cone coil (Magstim Company Limited, OHR Wales, UK; outside diameter of one half-coil, 12.5 cm; angle of two surfaces, 95°) connected to Magstim 200 stimulator (1.4 T at the coil surface when connected to Magstim 200) was used. We searched for the leg motor area during active contraction of the leg muscles. Subjects were asked to continuously contract the right tibialis anterior muscle with a constant force of approximately 50% of the maximum EMG output, which was fed back to the subjects by sound. The double-cone coil was then placed 2 cm anterior to the Cz. The stimulus intensity was increased from 20% of the maximum output in 5% steps until an MEP larger than 200 μV became just visible. The coil was then moved in 0.5-cm steps posteriorly or anteriorly and, if necessary, also medially or laterally, until the point of the maximum MEP was reached (the leg motor area). We then determined the active motor threshold (AMT), which was defined as the lowest stimulus intensity at which 5 out of 10 consecutive stimuli elicited a reliable MEP larger than 200 μV. We applied rTMS over SMA on the sagittal midline (Muri et al., 1994; Fink et al., 1997; Cunnington et al., 1996) with the active motor threshold intensity for the leg motor area. In the leg motor area, RMT is often not attainable in some subjects. Since AMT in the hand motor area is approximately 85% of RMT (Murase et al., 2005; Rounis et al., 2005), we chose the AMT for the leg muscle for stimulation of SMA.

In all conditions, the stimulation coil was held by hand. The coil position was marked on the head clearly with red ink to ensure accurate repositioning of the coil and was monitored continuously throughout the experiment. To confirm the anatomical position of the coil with regard to the subject's own cortical areas, we reproduced the anatomical TMS coil positions on the realistic cortex model-reconstructed MRI images using an image-guided TMS system (Brainsight: Magstim Co. Ltd., Carmarthenshire, Wales, UK) on 1 of 9 subjects (Fig. 1). In all of three conditions, the coils were found at appropriate anatomical positions.

SPECT

The perfusion SPECT images were measured before and after application of rTMS over PMC. Each subject received an injection of 555 MBq of 99mTc-ethylcysteinate dimer (ECD) via an intravenous line in order to avoid pain. Data acquisition was started 5 min after injection and performed with a double-head gamma camera (E.CAM Signature; SIEMENS, USA) with a total acquisition time of 7 min. Then, the subjects were given monophasic 0.2 Hz rTMS (250 pulses) over PMC. As soon as the application of rTMS finished, they received an injection of 99mTc-ECD and underwent SPECT studies again. During this session, the subjects lay supine on the scanning bed and were instructed not to move. The head of each subject was immobilized using a head holder.

Data were reconstructed so that images were converted into DICOM format after transfer to a workstation. All images were reconverted into ANALYZE format for statistical parametric mapping analysis and underwent normalization onto the template and smoothing using easy Z score imaging system (eZIS, version 2.0.0, developed by Matsuda H. of National Center of Neurology and Psychiatry, Mizumura S. of Nihon Medical University, Souma S. and Takemura N. of Daiichi Radioisotope Laboratory; Matsuda et al., 2004; Kanetaka et al., 2004). The differences in adjusted rCBF between before and after rTMS were determined by a voxel-by-voxel paired t test setting at height threshold (P = 0.001), uncorrected for independent multiple comparison. These differences were considered significant if they survived a correction for multiple comparisons with cluster level at P = 0.001 with the

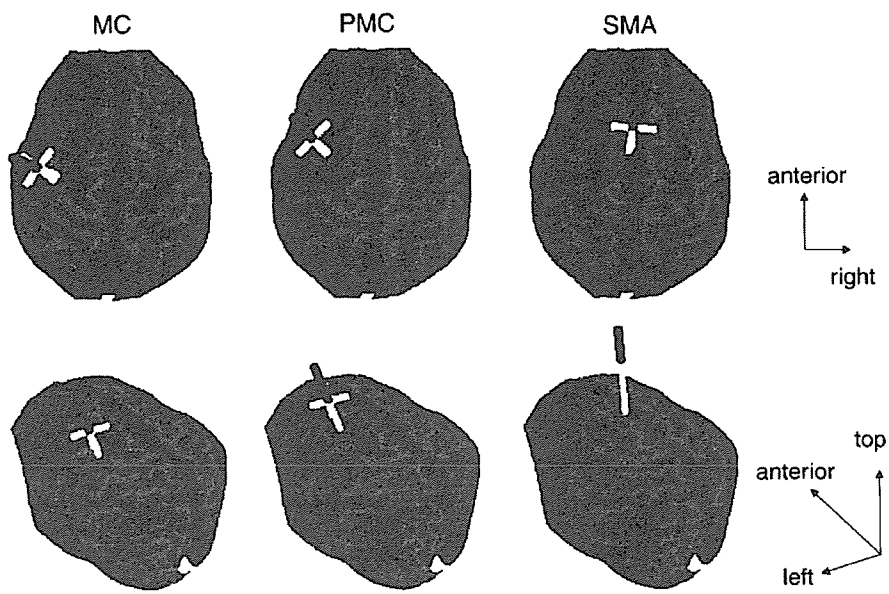

Fig. 1. TMS coil positions on realistic cortex model reconstructed MRI images from top (upper row) and left-sided back view (lower row). The cross-points of the yellow bars indicate the centers of the figure-of-eight or double-cone coils. The yellow bars indicate the sagittal and horizontal center lines of the coils to represent the horizontal plane of the coils. The red bars show the directions of the vertical axis through the center of each coil. The yellow lines as extended red lines are placed anatomically on each target area.

statistical parametric mapping software (SPM for windows, version 1.01, programmed by Sergey Pakhomov and Nick Tsygankov). The parametric maps were generated to determine significant regions of only increased activity because no regions reached significant decreases in activity. Then, the coordinates that reached the significance level in a MNI standard brain model were transformed into the Talairach and Tournoux coordinates (Talairach and Tournoux, 1988).

Statistical analysis of SEPs

We compared the aftereffects of rTMS between stimulation sites using the data from all 9 subjects who had SPECT studies. To evaluate the changes after rTMS, we subtracted SEP data before rTMS from those after rTMS for each measured component. These differences were analyzed by two-way repeated measures ANOVA using two factors: COMPONENT (latencies and amplitudes of each component) and SITE (stimulation sites at MC, PMC and SMA). When statistical significance is reached, we performed one-way repeated measures ANOVA using SITE as a factor to examine the stimulation site specific effects of rTMS. Post hoc comparison was carried out using Scheffe's F test.

Using the data from 6 of 9 subjects who participated in biphasic 1 Hz rTMS over PMC session, we compared the aftereffects of monophasic 0.2 Hz to biphasic 1 Hz rTMS over PMC. The differences between before and after rTMS were analyzed by two-way repeated measures ANOVA using two factors: COMPONENT and FREQUENCY (stimulation frequencies at 0.2 Hz and 1 Hz). When statistical significance is reached, paired t test was carried out for the examination of the stimulation frequency-specific effects and for the amplitudes of SEP components before and after rTMS. All data were analyzed with standard statistical software (Statview; SAS Institute, Cary, USA).

Results

SEPs

Fig. 2 shows the grand-averaged waveforms from 9 subjects. Because of the variations of latencies across the subjects, grand-averaged waveforms were constructed by adjusting the time to coincide the P14 peaks of each average. At both electrodes, the subcortical far-field P14 component was the first activity detected in all subjects. Table 1 shows the peak latencies and amplitudes of each component and their differences before and after application of monophasic 0.2 Hz rTMS over three cortical areas (MC, PMC, SMA).

The changes of *latencies* of median SEP components following rTMS showed no differences in two-way repeated measures ANOVA; SITE × COMPONENT ($F[16,128] = 0.930$, $P = 0.537$). In the *amplitudes* of SEP components, SITE × COMPONENT interaction was significant ($F[16,128] = 2.108$, $P = 0.012$), and one-way repeated measures ANOVA for these components using the factor of SITE (MC versus PMC versus SMA) was carried out. The factor of SITE was significant on two frontal negative components (N30: $F[2,16] = 10.257$, $P = 0.014$, N60: $F[2,16] = 3.765$, $P = 0.046$). Post hoc analysis was performed for these components. For N30 component, the amplitude change after application of monophasic 0.2 Hz rTMS over PMC was

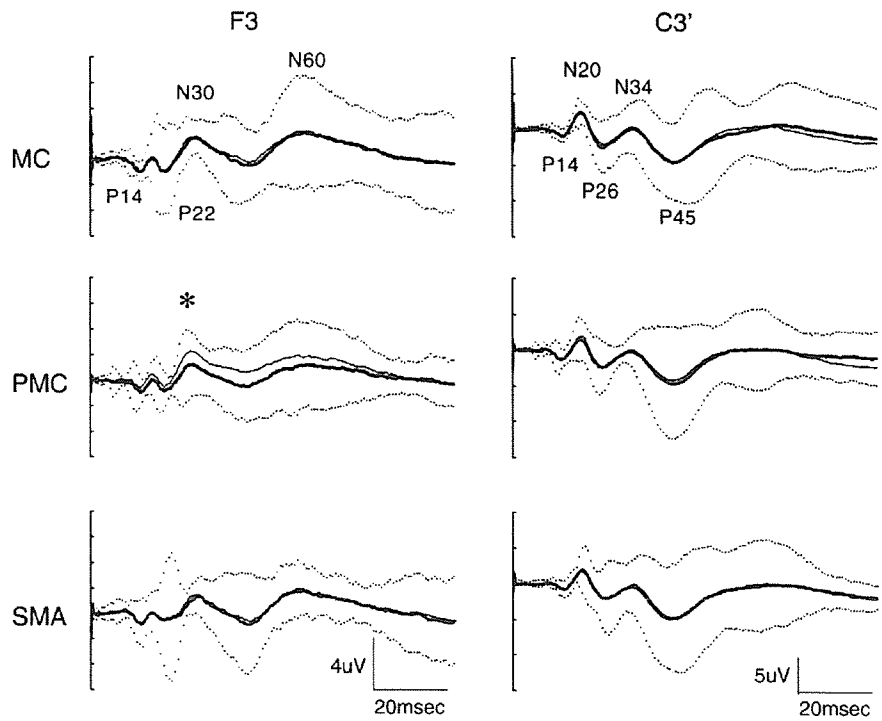

Fig. 2. Grand-averaged SEP waveforms from F3 (left column) and C3′ (right column) before (thick wave) and after (thin wave) application of monophasic 0.2 Hz rTMS over each stimulated site, MC, PMC and SMA. After application of rTMS over MC or SMA, no major changes occurred in SEPs, whereas significant increase in amplitude of N30 component (asterisk) was observed after application of rTMS over PMC. Dotted lines show 95% confidence interval of each SEP waveform recorded before rTMS.

Table 1
Peak latencies (a) and amplitudes (b) of each SEP component before and after application of rTMS over MC, PMC or SMA

(a) Latency (ms)

F3

	P14			P22			N30			N60		
	Before	After	Δ	Before	After	Δ	Before	After	Δ	Before	After	Δ
MC	13.7 ± 0.76	13.7 ± 0.97	0.0 ± 0.40	20.0 ± 1.37	20.2 ± 1.48	0.1 ± 0.36	28.6 ± 2.70	29.1 ± 2.69	0.5 ± 0.54	59.3 ± 3.45	58.6 ± 3.96	−0.8 ± 2.12
PMC	13.8 ± 0.90	13.5 ± 0.82	−0.3 ± 0.37	20.0 ± 1.23	20.0 ± 1.01	−0.0 ± 0.85	28.4 ± 1.98	28.4 ± 2.76	−0.0 ± 1.94	58.3 ± 4.95	57.5 ± 3.88	−0.8 ± 2.50
SMA	13.7 ± 0.82	13.9 ± 0.84	0.2 ± 0.32	20.1 ± 1.64	20.6 ± 1.66	0.5 ± 0.82	29.3 ± 3.27	28.9 ± 3.40	−0.4 ± 1.69	56.0 ± 3.45	56.7 ± 3.25	0.7 ± 3.11

C3′

	P14			N20			P26			N34			P45		
	Before	After	Δ	Before	After	Δ	Before	After	Δ	Before	After	Δ	Before	After	Δ
MC	13.8 ± 0.76	13.7 ± 0.99	−0.1 ± 0.43	18.9 ± 0.86	18.9 ± 1.29	−0.1 ± 0.51	24.6 ± 1.22	25.0 ± 1.16	0.4 ± 0.74	33.2 ± 1.31	33.3 ± 1.32	0.1 ± 1.30	45.0 ± 3.01	44.4 ± 2.74	−0.6 ± 1.49
PMC	13.8 ± 0.85	13.7 ± 0.90	−0.1 ± 0.27	19.1 ± 0.91	19.1 ± 0.77	0.1 ± 0.20	24.9 ± 1.47	24.6 ± 1.24	−0.3 ± 0.63	32.3 ± 2.00	32.5 ± 1.70	0.2 ± 1.59	43.7 ± 2.01	43.8 ± 1.84	0.1 ± 1.28
SMA	13.8 ± 0.77	14.2 ± 0.77	0.4 ± 0.40	19.1 ± 0.88	19.1 ± 0.78	0.1 ± 0.32	24.8 ± 1.46	24.9 ± 1.32	0.1 ± 0.60	32.4 ± 1.58	32.9 ± 1.81	0.5 ± 1.32	44.2 ± 2.17	44.6 ± 2.00	0.4 ± 1.41

(b) Amplitude (μV)

F3

	P14			P22			N30			N60		
	Before	After	Δ	Before	After	Δ	Before	After	Δ	Before	After	Δ
MC	1.17 ± 0.27	1.21 ± 0.45	0.05 ± 0.44	1.57 ± 1.67	1.18 ± 1.30	−0.40 ± 0.70	−2.14 ± 0.63	−2.11 ± 0.87	−0.03 ± 0.51	−2.58 ± 1.65	−2.60 ± 1.77	0.02 ± 0.67
PMC	1.30 ± 0.39	1.21 ± 0.55	−0.09 ± 0.36	1.13 ± 0.87	0.89 ± 0.63	−0.24 ± 0.66	−1.64 ± 1.31	−2.52 ± 1.53	**0.88 ± 0.55**	−1.82 ± 1.42	−2.65 ± 1.34	0.83 ± 0.51
SMA	1.22 ± 0.69	1.15 ± 0.66	−0.07 ± 0.40	1.32 ± 1.75	1.44 ± 1.96	0.12 ± 0.57	−1.75 ± 0.58	−1.95 ± 0.63	0.20 ± 0.32	−2.56 ± 2.28	−2.27 ± 1.09	−0.29 ± 1.11

C3′

	P14			N20			P26			N34			P45		
	Before	After	Δ	Before	After	Δ	Before	After	Δ	Before	After	Δ	Before	After	Δ
MC	1.17 ± 0.51	1.07 ± 0.44	−0.10 ± 0.41	−2.76 ± 1.24	−2.79 ± 1.13	0.03 ± 0.64	2.88 ± 2.25	2.70 ± 1.55	−0.18 ± 0.58	−0.58 ± 1.80	−0.88 ± 1.98	0.30 ± 0.61	4.94 ± 2.37	4.53 ± 3.15	−0.41 ± 1.52
PMC	1.33 ± 0.39	1.21 ± 0.38	−0.12 ± 0.12	−2.37 ± 0.80	−2.62 ± 0.90	0.25 ± 0.44	2.89 ± 1.84	2.96 ± 2.28	0.08 ± 0.74	−0.29 ± 0.84	−0.58 ± 1.28	0.28 ± 0.74	5.24 ± 3.18	4.78 ± 2.90	−0.46 ± 0.99
SMA	1.07 ± 0.43	1.07 ± 0.37	0.01 ± 0.35	−2.29 ± 0.89	−2.42 ± 0.94	0.13 ± 0.44	2.82 ± 2.16	2.83 ± 2.00	0.01 ± 0.73	−0.05 ± 1.64	−0.29 ± 1.53	0.34 ± 0.61	5.02 ± 3.61	4.88 ± 3.32	−0.14 ± 0.56

Values are expressed as mean ± standard deviation. Δ indicates subtraction of values before from those after rTMS. Bold figures show the significantly increased value after rTMS over PMC than MC or SMA.

significantly larger than that after MC stimulation ($P = 0.021$) or SMA stimulation ($P = 0.014$). But, N60 amplitude change after application of monophasic 0.2 Hz rTMS over PMC was not different from after MC stimulation ($P = 0.201$) and SMA stimulation ($P = 0.053$).

In addition, to confirm whether this PMC rTMS aftereffect on median SEP is specific in very low-frequency (monophasic 0.2 Hz) rTMS or not, we compared the aftereffects of monophasic 0.2 Hz rTMS over PMC on median SEP to biphasic 1 Hz rTMS in 6 of 9 subjects (Fig. 3 and Table 2). The changes of *latencies* of median SEP components following rTMS at both frequencies showed no differences in two-way repeated measures ANOVA: FREQUENCY × COMPONENT ($F[8,40] = 0.281$, $P = 0.969$). In the *amplitudes* of SEP components, FREQUENCY × COMPONENT interaction was significant ($F[8,40] = 3.740$, $P = 0.024$). The significant differences between the aftereffects of monophasic 0.2 Hz and biphasic 1 Hz rTMS were found for frontal N30 ($P = 0.022$) and N60 ($P = 0.012$) components and parietal N34 ($P = 0.020$) component by paired t test. However, the amplitude differences before and after rTMS were not significant for the parietal N34 ($P = 0.27$) in contrast with frontal N30 ($P = 0.002$) and N60 ($P = 0.029$). Therefore, the changes of these frontal components after monophasic 0.2 Hz stimulation were significantly larger than those after biphasic 1 Hz stimulation, and the differences were significant in frontal N30 and N60 only after monophasic 0.2 Hz stimulation.

We also recorded median SEPs using a 62-electrode cap system in 2 subjects. Topographical mapping at N30 latency demonstrated frontal N30 enhancement after application of monophasic 0.2 Hz rTMS over PMC, whereas parietal positive components were unchanged (Fig. 4), suggesting that SEP changes by rTMS occurred mainly at the frontal radial component rather than the tangential component as discussed below.

SPECT

The analyses of SPECT images revealed significant increases of cerebral blood flow in several regions after application of monophasic 0.2 Hz rTMS over PMC, whereas there were no regions with significant decreases. Fig. 5 shows areas with significant changes in cerebral blood flow after rTMS, and Table 3 shows their exact coordinates. These areas showing significant increases in blood flow included the regions, left middle frontal gyrus and precentral gyrus, under and near the magnetic coil (Fig. 5). These gyri correspond to areas 9 and 6 in Brodmann cytoarchitectural map of the human brain and include PMC and prefrontal cortex. An additional region showing blood flow increase was the cingulate gyrus.

Discussion

In the present study, we compared median SEPs before and after application of monophasic very low-frequency subthreshold rTMS over the primary and non-primary motor cortices. Application of monophasic 0.2 Hz rTMS over PMC, but not over MC or SMA, significantly increased the amplitude of frontal N30 component, but not of the parietal counterpart, and this effect was not seen after biphasic 1 Hz rTMS over PMC. This change was associated with increased rCBF in PMC and prefrontal cortex, as confirmed using SPECT imaging analysis. Using the same stimulation parameters as those in this study, we have shown that subthreshold monophasic very low-frequency rTMS over PMC, but not over MC or SMA, significantly improved symptoms of writer's cramp (Murase et al., 2005). The present findings corroborate these clinical effects specifically seen after PMC stimulation.

SEP waveforms before rTMS were slightly different among sessions of stimulating over MC, PMC and SMA (Fig. 2) or stimulation over PMC at monophasic 0.2 Hz and biphasic 1 Hz (Fig. 3) performed at least 1 week apart. This is probably due to the technical difficulty of reproducing the same recording electrode position. The comparison of waveforms before and after rTMS, the main analysis in this study, was free from this problem because the electrodes were kept attached to the scalp during the sessions. Although the coil positions were confirmed anatomically, it is conceivable that stimulation over PMC may have spread to MC or

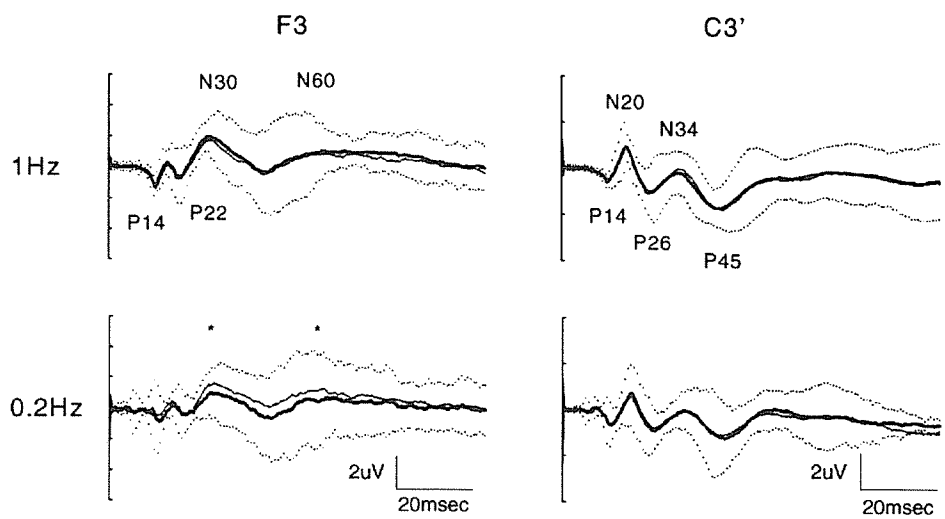

Fig. 3. Grand-averaged SEP waveforms from F3 (left column) and C3′ (right column) before (thick wave) and after (thin wave) application of rTMS over PMC at each stimulation frequency, biphasic 1 Hz and monophasic 0.2 Hz in 6 of 9 subjects. Asterisks show that the components showed larger aftereffects of monophasic 0.2 Hz than biphasic 1 Hz rTMS over PMC. Dotted lines show 95% confidence interval of each SEP waveform recorded before rTMS.

Table 2
Peak latencies (a) and amplitudes (b) of each SEP component before and after application of rTMS over PMC at monophasic 0.2 Hz or biphasic 1 Hz

(a) Latency (ms)

	F3											
	P14			P22			N30			N60		
	Before	After	Δ	Before	After	Δ	Before	After	Δ	Before	After	Δ
0.2 Hz	13.4 ± 0.85	13.1 ± 0.81	−0.3 ± 0.32	19.7 ± 1.20	19.6 ± 0.66	−0.1 ± 1.09	28.4 ± 1.89	27.3 ± 2.32	−1.0 ± 1.62	57.3 ± 4.87	56.2 ± 3.40	−1.0 ± 3.07
1 Hz	13.3 ± 0.86	13.5 ± 1.12	0.2 ± 0.74	20.0 ± 0.67	20.2 ± 1.22	0.2 ± 1.47	27.9 ± 1.99	27.4 ± 1.36	−0.6 ± 1.52	61.4 ± 7.55	61.8 ± 8.03	0.4 ± 4.32

	C3′														
	P14			N20			P26			N34			P45		
	Before	After	Δ	Before	After	Δ	Before	After	Δ	Before	After	Δ	Before	After	Δ
0.2 Hz	13.5 ± 0.90	13.4 ± 0.89	−0.2 ± 0.20	18.7 ± 0.70	18.8 ± 0.65	0.1 ± 0.18	24.9 ± 0.78	24.8 ± 0.90	−0.1 ± 0.46	32.7 ± 1.84	32.4 ± 1.57	−0.3 ± 1.79	43.1 ± 2.09	43.2 ± 1.97	0.1 ± 0.99
1 Hz	13.4 ± 1.01	13.9 ± 0.95	0.5 ± 0.65	18.7 ± 0.71	18.8 ± 0.73	0.1 ± 0.10	24.4 ± 1.39	24.6 ± 1.04	0.2 ± 0.40	31.5 ± 2.48	32.1 ± 2.36	0.6 ± 1.29	42.9 ± 2.79	43.7 ± 2.63	0.8 ± 0.91

(b) Amplitude (μV)

	F3											
	P14			P22			N30			N60		
	Before	After	Δ	Before	After	Δ	Before	After	Δ	Before	After	Δ
0.2 Hz	1.31 ± 0.42	1.11 ± 0.24	−0.20 ± 0.26	0.74 ± 0.59	0.72 ± 0.65	−0.01 ± 0.19	−1.49 ± 0.79	−2.09 ± 0.69	**0.61 ± 0.24**	−1.32 ± 1.06	−2.11 ± 0.68	**0.78 ± 0.63**
1 Hz	1.37 ± 0.35	1.45 ± 0.27	0.08 ± 0.38	0.84 ± 0.89	1.01 ± 0.88	0.17 ± 0.28	−2.19 ± 0.62	−2.02 ± 0.89	−0.18 ± 0.44	−1.80 ± 0.73	−1.53 ± 0.65	−0.27 ± 0.38

	C3′														
	P14			N20			P26			N34			P45		
	Before	After	Δ	Before	After	Δ	Before	After	Δ	Before	After	Δ	Before	After	Δ
0.2 Hz	1.41 ± 0.13	1.27 ± 0.15	−0.15 ± 0.12	−2.51 ± 0.49	−2.55 ± 0.78	0.04 ± 0.35	2.57 ± 1.56	2.50 ± 1.53	−0.07 ± 0.49	−0.19 ± 0.98	−0.23 ± 1.55	0.04 ± 0.85	4.06 ± 1.12	3.76 ± 1.52	−0.31 ± 1.02
1 Hz	1.51 ± 0.38	1.40 ± 0.10	−0.10 ± 0.44	−2.71 ± 1.06	−2.87 ± 0.96	0.16 ± 0.25	2.84 ± 1.62	2.90 ± 1.82	0.05 ± 0.86	−0.23 ± 1.16	0.14 ± 1.70	−0.36 ± 0.72	4.74 ± 1.14	4.83 ± 1.87	0.09 ± 0.95

Values are expressed as mean ± standard deviation. Δ indicates subtraction of values before from those after rTMS. Bold figures show the significantly increased value after monophasic 0.2 Hz than biphasic 1 Hz rTMS over PMC.